

Minimal Representation of Electrocardiogram Signals: Towards Low-cost Telecardiology

Roopak Rajendra Tamboli

A Thesis Submitted to
Indian Institute of Technology Hyderabad
In Partial Fulfillment of the Requirements for
The Degree of Master of Technology



Department of Electrical Engineering

January 2015

Declaration

I declare that this written submission represents my ideas in my own words, and where ideas or words of others have been included, I have adequately cited and referenced the original sources. I also declare that I have adhered to all principles of academic honesty and integrity and have not misrepresented or fabricated or falsified any idea/data/fact/source in my submission. I understand that any violation of the above will be a cause for disciplinary action by the Institute and can also evoke penal action from the sources that have thus not been properly cited, or from whom proper permission has not been taken when needed.

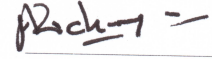
Roopak
09/01/2015
(Signature)

(Roopak Rajendra Tamboli)

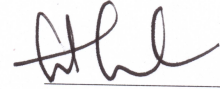
eellm/3
(Roll No.)

Approval Sheet

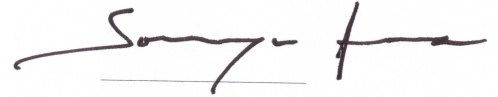
This Thesis entitled Minimal Representation of Electrocardiogram Signals: Towards Low-cost Telecardiology by Roopak Rajendra Tamboli is approved for the degree of Master of Technology from IIT Hyderabad



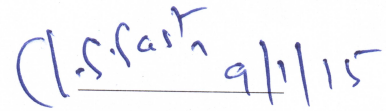
(Dr. Ashutosh Richhariya) Examiner
L. V. Prasad Eye Institute
Hyderabad



(Dr. Sumohana Channappayya) Examiner
Department of Electrical Engineering
IIT Hyderabad



(Dr. Soumya Jana) Adviser
Department of Electrical Engineering
IIT Hyderabad



(Dr. C. S. Sastry) Chairman
Department of Mathematics
IIT Hyderabad

Acknowledgements

I sincerely express my gratitude to everyone who supported me throughout the course of this work. I am thankful to my advisor Dr. Soumya Jana for his aspiring guidance, invaluable constructive criticism and friendly advice during the work. I am also thankful to Dr. C. S. Sastry, Dept. of Mathematics for his guidance on several issues related to the thesis.

A significant part of this thesis was benefited from the discussions that took place in the weekly meetings of Cyber Physical Systems Healthcare project at IIT Hyderabad. I am thankful to all the participants of those meetings, especially Dr. Amit Acharyya, Dr. Asudeb Dutta and Dr. K. Sri Rama Murty who attended the presentations and shared their views from time to time.

I am also thankful to my friends at IIT Hyderabad. Although it is not possible to mention all of them, D. S. Srikanth Reddy and B. Sandeep Chandra deserve a special mention for the enormous amount of help they have provided.

Finally, I thank Dr. Ramachandra Manthalkar, Shri Guru Govind Singhji Institute of Engineering and Technology, for the discussion related to sparse representation of electrocardiograms.

Dedication

To my family and to everyone who has been part of my learning experiences.

Abstract

This thesis seeks methods for minimal linear representation and subsequently low rate sampling of electrocardiogram (ECG) signals. ECG, a non-invasive approach to record heart's electrical activity, has been an ubiquitous tool for preliminary as well as complicated diagnoses of heart related issues. The modern lifestyle of ever increasing population has elevated the rate of heart diseases. Many a times, periodic monitoring of ECG, such as holter monitors, becomes imperative for diagnosis and curing of heart conditions. Some of the major issues in maintaining quality of healthcare services are low doctor to patient ratio in urban as well as resource constrained rural localities, unavailability of trained medical professionals in remote areas, infrastructural constraints etc. In this backdrop, personalized and mobile healthcare, such as telecardiology has been proposed.

In order to realize a resource friendly telecardiology system, several engineering aspects need attention. This thesis focuses on a few related signal processing issues. Specifically, compact representation and low rate sampling of ECG signals, subject to certain representation/ reconstruction accuracy are discussed. It is observed that 'sym4' and 'db4' wavelets pack the energy of various ECG signals in least number of coefficients. Further, the proposed hybrid Fourier/ wavelet method is shown to offer even sparser representation by using Fourier approximation for the low frequency component and wavelet approximation for the remaining part of the signals. The former contains most of the signal energy whereas the latter accounts for key clinical information at feature points. Next, sparsity of ECG signals is exploited to demonstrate near universality of the proposed nonuniform sampling scheme. Recent advances in compressive sensing (CS) theory have facilitated recovery from samples acquired in a nonuniform manner.

The evaluation of proposed methods is based on empirical studies on large ECG datasets available publicly. This is justified as proposing a statistical model for ECG signals is difficult on account of wide variety of such signals. Objective quality measures are used to judge the performance.

Contents

Declaration	ii
Approval Sheet	iii
Acknowledgements	iv
Abstract	vi
Nomenclature	viii
1 Introduction	1
1.1 Scope of the Thesis	2
1.2 Literature Survey	3
1.3 Evaluation Methodology	5
1.3.1 ECG Datasets	5
1.3.2 Quality Measures	6
2 Sparse Representation of Electrocardiograms	7
2.1 Some Characteristics of ECG Signals	7
2.2 ECG Approximation: Theoretical Context	8
2.3 Choice of Wavelet for Sparsest Representation	9
2.3.1 Experimental data generation	9
2.3.2 Results	10
2.4 A Hybrid Fourier/ Wavelet Technique for ECG Approximation	10
2.4.1 Proposed Algorithm	12
2.4.2 Experimental Data Generation	13
2.4.3 Results	14
2.5 Comparison of Hybrid Approximation Method with other Representation Methods .	16
3 Low-rate Sampling of ECG Signals	19
3.1 Compressive Sampling of ECG Signals	20
3.1.1 Targetted OMP (TOMP)	20
3.1.2 Compressive Sampling of ECG Signals using Random Measurement Matrices	21
3.2 Universal Nonuniform Sampling Scheme for ECG	22
3.2.1 Experiments	23
3.2.2 Results	23

4	Summary and Discussion	27
4.1	Sparse Representation	27
4.2	Reduction in Sampling Rates	28
A	Theoretical Background	29
A.1	Sampling	29
A.2	Dimensionality Reduction Problem	30
A.3	Compressive Sensing	31
A.3.1	Restricted Isometry Property (RIP)	32
A.3.2	Greedy Reconstruction Algorithms	32
A.4	Dictionary Learning	32
	References	33

Chapter 1

Introduction

Heart related diseases such as arrhythmias are a leading cause of deaths across the world. An indispensable tool in diagnosing, monitoring and managing such diseases is the *electrocardiogram (ECG)*, which is a noninvasive record of heart's electrical

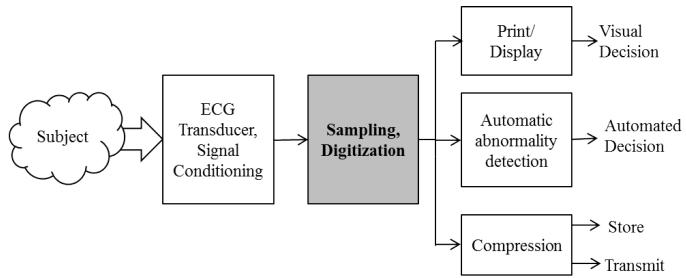


Figure 1.1: Schematic of a Generic ECG equipment

activity. Not surprisingly, the impact of heart diseases is especially severe in developing countries, where the high cost of ECG machines remains an impediment towards satisfactory disease management [1]. Compounding the challenge, grid electricity is generally erratic in the worst-affected (remote) locations, which necessitates low-power operation that can be sustained even via sporadic access to grid power. Further, on account of low doctor-to-patient ratio and unavailability of trained medical professionals, telecardiology appears to be a promising solution. Telecardiology involves acquisition and transmission of electrocardiogram (ECG) signals to a remote facility, where diagnosis is performed towards possible intervention. Unfortunately, the far flung population, who are perhaps in the biggest need of telecardiology, are often under-privileged and have limited access even to nominal infrastructure such as bandwidth and power. In such circumstances, it becomes imperative to design healthcare systems taking infrastructural constraints into account. Note that one can reduce storage and transmission requirements by compressing ECG signals. In dire circumstances, where inadequate power makes intensive compression algorithms infeasible, one may adopt the low-power alternative of compressive sampling, albeit sacrificing some compression efficiency.

Central to this discussion lies the ECG equipment. A classical ECG machine, where cardiac activity is picked up by an electrode (or multiple electrodes), and continuously recorded on a roll of paper, does not fit in the scope of thesis, as it requires high operational power arising from continuous operation, and motorized recording. In today's digital era, ECG records are increasingly being maintained in electronic form, and machines directly producing digitized ECG signals have become commonplace. As depicted in figure 1.1, a digital ECG equipment picks up the underlying analog signal using appropriate transducers, conditions it suitably, samples and converts it to the digital form using an analog-to-digital converter [2]. The digital data can then be printed or displayed for diagnosis of potential abnormalities by medical professionals. Those data can also be used for

automated decision making. Very often, such signals are stored locally, or transmitted to a remote location, respectively, for decision making at a later point, or at a distance. Accordingly, with a view to minimize storage requirement and/or communication bandwidth, one desires to represent ECG signals as compactly as possible without adversely affecting eventual clinical interpretation.

In the long run, a field-deployable system is envisioned that (i) records only the minimal amount of data, which are adequate for faithful reconstruction of the original ECG signal, and (ii) operates at an extremely low power. For example, one may introduce a resource friendly Holter monitor which is generally a small, portable, battery-powered medical device. It is employed when a doctor needs more information about the functioning of heart than a routine electrocardiogram. Holter monitoring refers to a 24-hour, continuous test to record your heart rate and rhythm. A patient wears the Holter monitor for 12 to 48 hours as they go about their normal daily routines. Its typical use would be in a health drive for collection of ECG data from large rural populations living away from the power grid. The ultra-low-power requirement would obviate the need to either carry a weighty load of electrical cells, or to make frequent trips to a charging station which may be far away. The reconstruction algorithm does not run on portable system, which only collects data sufficient for later reconstruction. Such data are transferred to a resource-rich central facility, where the reconstructed signal is obtained by a potentially complex algorithm.

1.1 Scope of the Thesis

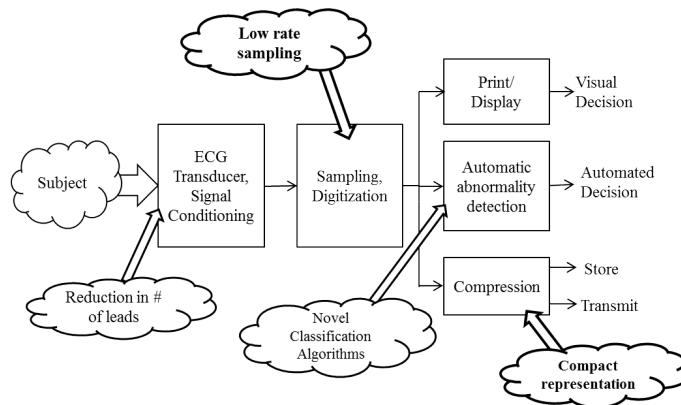


Figure 1.2: Low cost ECG: Some of the engineering opportunities and scope of the thesis

Figure 1.2 depicts several ways to realize low cost telecardiology with the help of a generic ECG equipment. Those include (i) reduction in number of leads in an ECG equipment making it portable, (ii) classifying ECG signals into normal and abnormal classes prior to transmission, (iii) ECG compression and (iv) low rate sampling. For example, Chandra et al. have presented a system level study on how classification of ECG based on Hurst exponent is instrumental in saving resources [3]. Maheshwari et al. have presented a study on reduced lead system selection methodology for reliable standard 12-lead reconstruction targeting personalized remote health monitoring applications [4].

The focus of this thesis is on minimal linear representation of electrocardiogram signals and applications that are benefited with such minimal representation (highlighted clouds in figure 1.2). Detailed problem description in mathematical terms is discussed in the next chapter. It is imperative

to study the properties of ECG signals that help achieving aforementioned goals. Towards this, various analyses of ECG signals in Fourier and wavelet domain are presented in chapter 2, followed by some results on choice of wavelets for sparsest representation of ECG signals. Taking one step further, hybrid Fourier/ wavelet approximation is shown to represent ECG signals even more succinctly, with certain cost involved. Next, various transform based representations of ECG signals are compared. Further, chapter 2 also shows a comparison among proposed hybrid scheme, representations using overcomplete dictionaries, wavelet bases, discrete cosine transform and Karhunen-Loeve (KL) bases derived from the signals. Next, chapter 3 presents the second area of focus, namely low rate sampling of ECG signals. First, compressive sampling of ECG signals with random measurement matrices is presented in brief. Next, near-universality of proposed nonuniform sampling of ECG signals, using measurement matrices that are row-restrictions of identity matrices is presented. Finally, chapter 3 presents some closing remarks and future scope.

1.2 Literature Survey

As discussed in the previous section, this thesis studies minimal linear representations of ECG signals and corresponding applications. The literature available in this context can roughly be divided into a few categories such as (a) compression of ECG signals exploiting their properties in time domain, (b) transform coding based compression that includes discrete wavelet transform (DWT), discrete cosine transform (DCT), Karhunen-Loève transform (KLT) and dictionary based representations, (c) adaptive sampling schemes for low-rate telecardiology, (d) compressive sensing (CS) of ECG for compression and (e) finally compressive sampling for low-power telecardiology. In addition to these, a few researchers also discuss impact of sampling rates on diagnostic quality and accordingly suggest objective quality measures for evaluation of algorithms that operate on ECG signals. Although this thesis does not propose any compression algorithm, the related literature is studied to some extent as it gives useful insights for finding efficient representation methods.

To begin with, importance of minimal representation for various applications is discussed. Next, utility of CS in the context of envisaged low-cost, low-power telecardiology is reviewed. A significant amount of the literature employing CS for ECG focuses on telecardiology applications, especially in ambulatory environments. Such approaches are reviewed in [5]. As explained in detail elsewhere (appendix A) in this thesis, success of CS depends on three key factors, namely, the measurement operator, signal sparsity and recovery scheme. It is necessary that the signal under consideration assumes sparsity, either in signal (time/ spatial) domain or in some transformed domain. The efficacy of the applications such as compression, denoising or compressive sampling, depends on signal sparsity. In compression, the sparsest representation provides the least dimension in which the signal space could be embedded. At the same time, such representation allows for the most efficient denoising, as well as perfect reconstruction from the least number of compressive samples. Further, the CS measurement or sampling operator performs non-adaptive (signal independent) linear measurements. It should be incoherent with the sparsifying transform. The CS recovery algorithm should be able to solve a large underdetermined system of linear equations under sparsity constraint. Having assured these key factors, further difficulty arises in the actual deployment where one acquires the signal in a random non-uniform manner rather than conventional uniform sampling.

ECG signal compression has been studied over several decades [6, 7]. Two main streams are

observed in the literature. The first one focuses on modeling and prediction in time domain. The other one studies transform based methods, using both fixed and adaptive bases. Both of these areas are reviewed to some extent.

Direct data compression techniques utilize prediction or interpolation algorithms. These techniques attempt to reduce redundancy in the data by examining a successive number of neighboring samples. A prediction algorithm utilizes a priori knowledge of some previous samples, while an interpolation algorithm employs a priori knowledge of both previous and future samples. One of the early methods for compression of the ECG by prediction or interpolation and entropy encoding appears in [8]. Baali et al. propose an approach that involves the projection of the excitation signal on the right eigenvectors of the impulse response matrix of the LPC filter. Each projected value is then weighted by the corresponding singular value, leading to an approximated sum of exponentially damped sinusoids [9]. An evaluation of various algorithms for real-time ECG data compression such as AZTEC(amplitude zone time epoch coding), TRIM (turning point/ recursive improvement), SAPA-2 (Scan-Along Polygonal Approximation) etc. is presented in [10, 11, 12, 13, 14].

A variety of compression algorithms represent ECG signals in suitable orthogonal basis and exploit signal redundancy in the transformed domain. Indeed, success of a compression algorithm depends on how compactly the signal is represented upon transformation. An ECG data compression method using Fourier descriptors is presented in [15]. The method is simple, requiring implementation of forward and inverse FFT. Ahmed et al. have studied ECG data compression with two specific orthogonal transforms, namely DCT and Haar transform [16]. These two representation are also compared with KLT. A more detailed study of KLT based representation for ECG appears in [17, 18]. Kiryu et al. present an early study on ECG data compression by biorthogonal basis and show that the performance is very similar to KLT [19]. Bendifallah et al. present an ECG compression method using DCT. A uniform scalar dead zone quantizer and arithmetic coding are the main components of the compression method proposed there.

Various researchers have reported ECG signals to be sparse in wavelet bases. In other words, only a few wavelet coefficients pack most of the signal energy. Benzid et al. have presented a study on fixed number of wavelet coefficients to be zeroed for ECG compression [20]. Review of wavelets in biomedical applications appears in [21]. Abo-Zahhad et al. present ECG compression algorithm based on coding and energy compaction of wavelet coefficients [22]. It generates a binary stream that encodes the structure of wavelet coefficients. This stream is compressed using a modified run length encoding. In an earlier study, they attempt ECG compression based on the compression of the linearly predicted residuals of the wavelet coefficients [23]. Various researchers have observed signal sparsity in wavelet and related domains, and have demonstrated the respective efficacy of wavelet packets [24], SPIHT (set partitioning in hierarchical trees) algorithm [25], and in particular “Daubechies 4” (db4) wavelet basis [26]. Adaptive/data-dependent basis selection for ECG signals based on machine learning has also been suggested. Tuzman et al. discuss design of wavelet basis for ECG data compression [27, 28]. However, the simplicity of a fixed basis is attractive in various applications. Indeed, empirical studies on wavelet basis selection have been carried out for compression as well as denoising [29, 30]. Such studies either narrowly target one wavelet family, or consider limited number of ECG signals, or only one lead, thereby limiting their utility. An exhaustive empirical study on the choice of wavelets is presented in this thesis [31].

Signal sparsity also plays a crucial role in recent compressive sensing (CS) based telecardiology

solutions [3, 32]. Other applications, such as denoising, are facilitated by sparsity. For example, a sparser representation allows more coefficients to fall below a threshold thus allowing more noise to be removed [33]. CS-based techniques have already proven effective in ECG signal compression [25, 34, 35, 36]. However, effectiveness of such techniques has been demonstrated for individual ECG signals. In other words, those are adapted to specific signals, and their effectiveness as a universal tool remains unknown. In contrast, this work proposes a low-power ECG recorder (the shaded block in figure 1.1) that would perform well for any ECG signal [37].

1.3 Evaluation Methodology

It is a common practice to evaluate algorithms using standardized datasets of ECG signals. The most popular database across various research areas focused on ECG is the Physionet database [42]. This thesis also uses three representative datasets, listed in table 1.1.

1.3.1 ECG Datasets

Table 1.1: Various datasets used in this thesis for experimental data generation [42]

Dataset	Sampling freq.(Hz)	Resolution (bits)	Availability of Lead-wise data	No. of patients	Annotations
PTBDB	1000	16	15 Leads [†]	290 (549 records)	NA
ANSI -AAMI	720	12	-	4	NA
Arrhythmia	360	11	2 Leads	48	Available

[†] 12 standard leads and 3 Frank - X, Y, Z leads

A variety of standard ECG signals from several patients are made available by Physionet database [42]. It includes records from subjects with different disease conditions and age groups. In this work, three representative databases have been used for experimental data generation. Table 1.1 provides information on databases used. Although beatwise annotations are not available, PTB database has provided labels indicating disease classes. The distribution of said 290 patients is as follows: myocardial infarction - 148, cardiomyopathy/ heart failure - 18, bundle branch block - 15, dysrhythmia - 14, myocardial hypertrophy - 7, valvular heart disease - 6, myocarditis - 4, miscellaneous - 4 and healthy controls - 52. Similarly, ANSI/AAMI EC13 test waveforms represent the extremes among ECG signals, and are used for testing the functioning of cardiac devices. In this database, there are four natural ECG records, namely, *aami3a*, *aami3b*, *aami3c* and *aami3d*, corresponding the respective cardiac conditions, ventricular bigeminy, slow alternating ventricular bigeminy, rapid alternating ventricular bigeminy, and bidirectional systoles. Other signals in the database are synthetic, and are not considered here.

An ECG signal from a database is record of heart activity for several minutes. For example, typical length of a record exceeds 40000 samples (shown in figure 1.3). For the purpose of experimental data generation, snippets of certain length are taken into account, instead of one complete record. Length of such snippets is chosen from the set {256, 512, 1024, 2048, 4096} (in samples), depending upon the application. Some overlap is maintained between two such snippets. These signal snippets are mentioned as ‘signal’ henceforth.

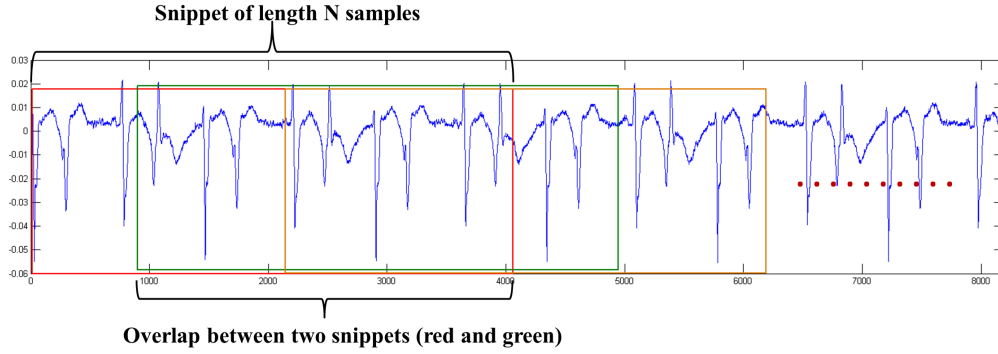


Figure 1.3: Generating snippets from the ECG records

1.3.2 Quality Measures

For an ECG signal $x(t)$, where $t \in \mathcal{R}$, a digital ECG machine produces a digital signal $x\{t_i\}$, where $i \in \mathcal{Z}$. For simplicity, denote it by x . An algorithm takes $x \in \mathcal{R}^N$ as input, where $N \in \{256, 512, 1024, 2048, 4096\}$, and produces \hat{x} . This \hat{x} can be one of the following: an approximated version of x , decompressed version of compressed x , recovered from low-rate samples of x or denoised version of the received noisy x . The related algorithm is evaluated using some performance evaluation criteria. In most of the cases, such a criterion is measuring the distance between x and \hat{x} using some distance measure d . It is necessary that such objective measure is in accordance with the doctors' opinion, for which researchers resort to mean opinion scores (MOS) collection [43, 44, 45, 46].

This work uses R^2 statistics as a quality measure to evaluate proposed methods [2]. The R^2 measure between x and \hat{x} is defined by

$$R^2 = 1 - \frac{\|x - \hat{x}\|_2^2}{\|x - \bar{x}\|_2^2}. \quad (1.1)$$

Here, \bar{x} denotes the mean value of the signal x . The score is generally presented as a percentage. R^2 appears to be very similar to the popular percentage root-mean-squared difference (PRD). It is suggested that DC bias should be subtracted from the denominator term in PRD in order to avoid artificially lower values than the true measure [5]. R^2 is thus one minus PRD with mean subtracted from the denominator term. Note that a perfect reconstruction leads to 100% R^2 accuracy, and it is desirable to maintain high R^2 values.

At this point, notice that even if average signal accuracy (as measured by R^2) is high, error concentration at feature points could undermine the integrity of clinically relevant information. This indicates that high signal accuracy, only if accompanied by well distributed approximation error, would ensure integrity of clinical information. In other words, it is desirable to have an error distribution without heavy tail, and less variation in error variance taken over successive windows. For the sake of completeness, the variance of a discrete-time signal x is defined below

$$Var(x) = \frac{1}{N-1} \sum_{i=1}^N (x_i - \bar{x})^2. \quad (1.2)$$

Chapter 2

Sparse Representation of Electrocardiograms

The efficacy of applications such as compression, denoising or compressive sampling, depends on signal sparsity. In compression, the sparsest representation provides the least dimension in which the signal space could be embedded (see section A.2). At the same time, such representation allows for the most efficient denoising, as well as perfect reconstruction from the least number of compressive samples. This chapter explores a few ways to represent ECG signals in minimal number of transform coefficients. Initially, signal approximation problem is described mathematically and some properties of ECG signals have been studied. Next, cumulative energy packing by various wavelets has been studied, in order to find wavelet(s) that offer succinct representation. A major part of this chapter is dedicated for the proposed ECG approximation method, called as Hybrid Fourier/ wavelet approximation [47]. The concluding section compares hybrid approximation with various representations in well known orthogonal bases, as well as Karhunen-Loève (KL) basis and dictionary based representation.

2.1 Some Characteristics of ECG Signals

To begin with, relevant properties of ECG signals have been studied which in turn guide the design of efficient representation. As shown in figure 2.1a, Fourier spectrum of an ECG signal often possesses large number of significant components stretching up to an appreciably high frequency. In other words, the Fourier representation of ECG signals is generally not sparse. Further, signal approximation error using Fourier coefficients tends to accumulate near feature points (see figure 2.10(c)), undermining clinical fidelity. The two undesirable properties, namely, the lack of sparsity, and inappropriate error shaping, generally make Fourier approximation unattractive.

In this backdrop, it is necessary to examine the structure of ECG signals, which consists of a strong rhythmic (low-pass) component, and various temporally localized features (high-pass component). The former contains the lion's share of signal energy. Specifically, figure 2.1b depicts a conservative example, where 90% of the signal energy is packed only up to a frequency of about 30Hz. Interestingly, notwithstanding its lack of suitability for encoding the entire spectrum, Fourier analysis remains attractive for encoding such low-pass component. On the other hand, the the resid-

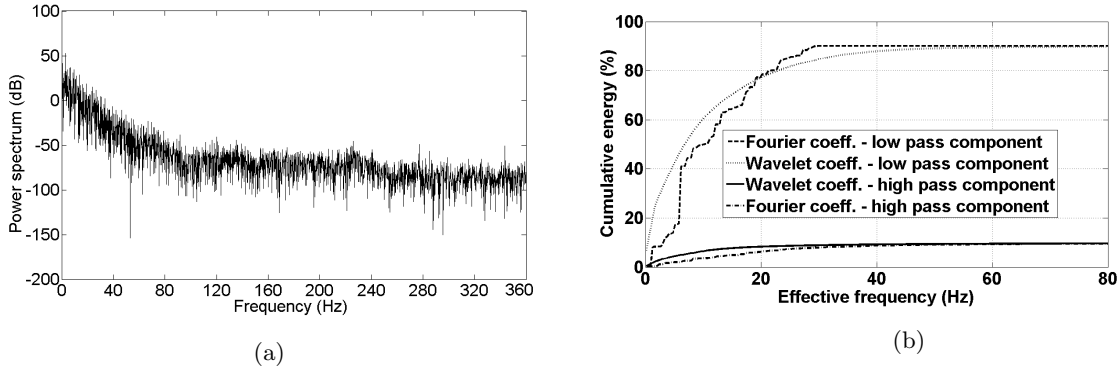


Figure 2.1: (a) Power spectrum of signal *aami3c*, (b) [Cumulative energy plot for *aami3c*:] Comparison of Fourier and wavelet techniques in terms of ECG energy packing.

ual high-pass component accounts for temporally localized features that are better represented by wavelets. Clearly, the latter component would require a far larger number of coefficients in a Fourier representation. In view of the above observation, an encoding algorithm is proposed that divides the ECG spectrum into low-pass and high-pass components as above, and use the Fourier and the wavelet methods respectively for their encoding. In this work, “db4” wavelet basis is used widely, in view of its reported superiority [26].

2.2 ECG Approximation: Theoretical Context

In the beginning the ECG signal approximation problem is placed in known theoretical context. In particular, the problem boils down to an minimum description length (MDL) problem with search space restrictions [48]. Consider set \mathcal{F} of ECG signals of length N . Intuitively, \mathcal{F} should be a relatively small subset of the set \mathcal{R}^N of all N -length signals. In the linear signal approximation problem, one assumes the existence of subspace Σ_K of dimension $K \ll N$ such that projection \hat{x} of any $x \in \mathcal{F}$ onto Σ_K provides an ϵ -accurate linear approximation, i.e., $\|x - \hat{x}\| < \epsilon\|x\|$ for small $\epsilon > 0$. Here $\|\cdot\|$ indicates norm generally, and the 2-norm specifically. One then seeks that subspace which achieves ϵ -accuracy with minimum K . In transform coding parlance, the above translates to the problem of identifying the optimal unitary transform U such that the minimum number K of transform coefficients provides ϵ -accuracy. In this framework, the same transform U is applied to each signal $x \in \mathcal{F}$, and the locations of the preserved coefficients are independent of x .

The aforementioned problem would simplify if ECG signals were to admit a statistical model. In such hypothetical scenario, one would view various observed signals as realizations of an underlying random vector $X \in \mathcal{R}^N$. In addition, if X were Gaussian, the optimal transform is known to be the Karhunen-Loève transform (KLT). Further, assuming the KLT coefficients are arranged in the descending order, one would keep the first K coefficients such that their energy is within a factor ϵ of the aggregate signal energy [49]. The optimality of KLT would still hold if the distribution of X belonged to the broader family of Gaussian scale mixtures, which is known to model a wide class of physical phenomena [50].

As alluded earlier, statistical approximation (based on stochastic averages) of ECG signals may not be appropriate, partly because many clinically significant ECG signals occur rather infrequently,

and their signature includes specific temporal features. This practical requirement is better served if the worst-case approximation performance over all ECG signals is held above a certain threshold. In this (deterministic) framework, a strictly linear method appears overly restrictive. Without such restriction, the problem reduces to an MDL problem [48]. Formally, given any $\epsilon > 0$, consider any function pair (ϕ, ψ) such that $z = \phi(x)$, $\tilde{x} = \psi(z)$, and $\|x - \tilde{x}\| \leq \epsilon$ for $x \in \mathcal{F}$. Further, record the worst-case (longest) description length of z by sweeping through all $x \in \mathcal{F}$. The (ϕ, ψ) pair for which the aforementioned worst-case description length is minimized, needs to be obtained.

Finding the optimal pair (ϕ, ψ) is known to be difficult. As a practical alternative, the optimal pair is sought over a smaller search space. In this context, the proposed hybrid Fourier/wavelet technique, where appropriate transform coefficients and their locations (only for wavelet) are retained, indeed imposes a specific structure on ϕ (and hence on ψ). In particular, referring to figure 2.5, the search for ϕ is conducted only by varying K_1 and K_2 , and wavelet coefficient locations through all possibilities.

2.3 Choice of Wavelet for Sparsest Representation

Figure 2.2: List of wavelets used

Wavelet Family	Biorthogonal and reverse biorthogonal (<i>biorM.N</i> , <i>rbioM.N</i>)	Symlets <i>symN</i>	Daubechies <i>dbN</i>	Meyer
Wavelets used	1.1, 1.3, 1.5, 2.2, 2.4, 2.6, 2.8, 3.1, 3.3, 3.5, 3.7, 3.9, 4.4, 5.5, 6.8	2 to 8	1 to 10	Meyer

As discussed in the literature survey, adaptive/data-dependent basis selection for ECG signals based on machine learning has been suggested several times. However, the simplicity of a fixed basis is attractive in various applications, especially in the context of low cost telecardiology, where cost of training a basis is not affordable. Indeed, empirical studies on wavelet basis selection that have been carried out so far either narrowly target one wavelet family, or consider limited number of ECG signals, or only one lead, thereby limiting their utility. In contrast, this work considers a large collection of wavelet bases including those from the Daubechies, Symlet, biorthogonal, and reverse biorthogonal families. The evaluation is performed on PTB Diagnostic ECG Database (see table 1.1).

2.3.1 Experimental data generation

An ECG signal x of length N is chosen to start with. Its N -point discrete wavelet transform (DWT) is computed using wavelet Ψ to obtain wavelet coefficients \tilde{x} . Next, let \tilde{y} contain first K significant coefficients from \tilde{x} , without altering their original locations. The remaining $N-K$ locations in \tilde{y}

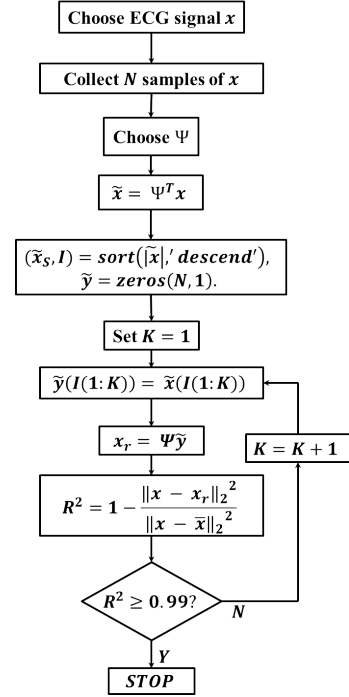


Figure 2.3: ECG approximation method

are set to zero. Then, a linear approximation x_r of the ECG signal x is obtained by performing Inverse DWT on \tilde{y} . The value of K is incremented in steps of 1 until the R^2 score, defined in (1.1), reaches 99%. This procedure is depicted in figure 2.3. In this study, all ECG signals from The PTB Diagnostic ECG Database from Physionet have been used without any pre-processing [42]. The database offers 549 signals from 290 subjects recorded at 1000 Hz. Each record contains information from standard 12 leads and 3 Frank leads making available over 8200 signals for analysis. Aforementioned steps are repeated for all the ECG signals in the database, where the aim is to find K for different leads and wavelet bases.

2.3.2 Results

Figure 2.4 compares average performance of best wavelet bases from the ‘Symlet’, ‘Daubechies’ and ‘Biorthogonal’ families, respectively, for fifteen leads. Notice that the highest sparsity is exhibited by ‘sym4’ (Symlet), which is closely followed by ‘db4’ (Daubechies), but far ahead of ‘bior1.1’ (biorthogonal). Interestingly, the aforementioned behavior remains more or less consistent across all fifteen leads. Even more remarkably, similar behavior is seen even across disease classes (not shown due to space constraints). A more exhaustive study is furnished in table 2.1. Wavelet bases which do not pack 99% of the signal energy (equivalent to achieving 99% R^2 score) within about $N/8$ coefficients are not shown (except Meyer wavelet). It is seen that energy compaction efficiency is more in lower order wavelets and decreases with increasing order, in case of Daubechies wavlets and symlets. Biorthogonal families which are popular in ECG denoising literature can not offer very sparse representation. In this process, an interesting observation made is the following: When considering all fifteen leads, ‘v1’ through ‘v6’ and ‘vx’ (Frank X) appear to admit sparser representation (figure 2.4). This could also guide efficient subset selection while reconstructing the full set of leads from a subset, a key to portable design.

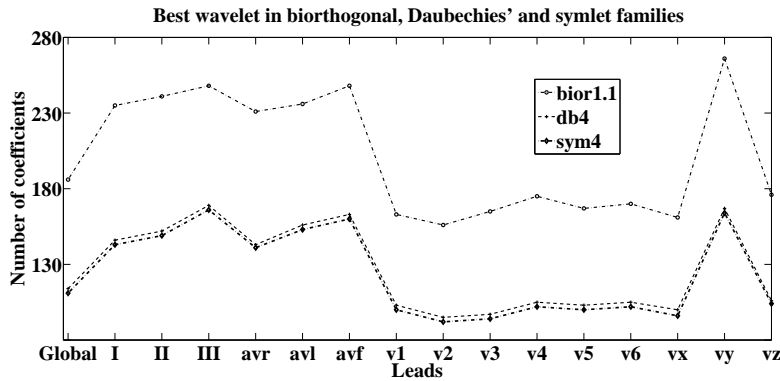


Figure 2.4: Averaged performance of selected wavelets across all leads.

2.4 A Hybrid Fourier/ Wavelet Technique for ECG Approximation

The proposed encoder, depicted in figure 2.5, is parameterized by three integers N , K_1 and K_2 . Specifically, N denotes the signal length. Further, the first K_1 coefficients of the N -point FFT of

Table 2.1: Averaged performance of various wavelets across all leads. Number of coefficients (K) is rounded to integer.

Wavelet	Leads														Overall	
	I	II	III	avr	avl	avf	v1	v2	v3	v4	v5	v6	vx	vy		vz
sym4	143	149	166	141	153	160	100	92	94	102	100	102	96	164	104	111
sym6	144	148	165	141	153	159	100	93	95	104	101	103	97	162	105	112
sym5	144	149	166	141	154	160	101	93	96	104	101	103	97	164	106	113
db4	146	152	169	143	156	163	103	95	97	105	103	105	100	167	106	114
sym8	145	149	165	142	154	159	103	95	97	105	103	105	100	163	107	114
db3	148	154	171	145	157	166	102	94	97	105	104	106	100	170	106	115
sym3	148	154	171	145	157	166	102	94	97	106	104	106	100	170	107	115
sym7	146	150	166	143	155	160	103	95	98	106	104	106	101	164	107	115
db5	149	154	171	146	159	165	106	98	101	109	107	109	104	169	109	118
db6	153	157	174	149	162	168	110	102	105	113	112	113	108	171	113	121
db2	157	164	181	155	166	176	107	99	103	112	109	111	104	183	113	122
sym2	157	164	181	155	166	176	107	99	103	112	109	111	104	183	113	122
db7	155	159	175	152	164	169	112	105	108	116	115	116	111	172	115	124
db8	158	161	177	155	167	171	115	108	111	119	119	119	115	175	118	127
db9	162	165	181	158	170	174	118	111	114	123	123	123	118	177	121	131
db10	165	168	184	161	173	177	122	114	117	127	126	127	122	180	124	134
bior1.1	235	241	248	231	236	248	163	156	165	175	167	170	161	266	176	186
rbio1.5	236	243	249	233	237	250	164	158	166	176	169	172	163	267	178	187
rbio1.3	236	243	250	233	238	250	164	158	166	176	168	172	163	267	178	188
bior4.4	363	322	337	320	351	324	212	233	244	231	201	206	189	371	246	241
rbio4.4	492	416	425	429	462	408	317	379	390	361	307	307	299	470	380	354
Meyer	977	987	990	982	985	991	964	961	964	965	964	971	957	986	967	968

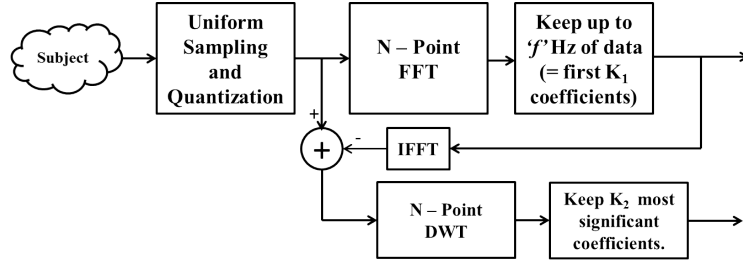


Figure 2.5: Conceptual block diagram of hybrid Fourier/wavelet encoder.

the signal are retained, which amounts to $2K_1$ numbers. Thus the parameter K_1 determines the cutoff frequency for the low-pass components. Next the corresponding low-pass signal, obtained via N -point inverse FFT (IFFT), is subtracted from the original, and the residual high-pass component remains. We take N -point discrete wavelet transform (DWT) of that residual, and retain K_2 most significant coefficients. However, such significant coefficients are expected to occur at isolated locations, which we also need to preserve. As a result, we end up with $2K_2$ numbers.

For the sake of simplicity, each number is assumed to be represented by a machine word, whose length is not optimized. The signal length N is also kept fixed. In this setup, the optimal pair (K_1, K_2) is sought such that the total number of retained numbers $2(K_1 + K_2)$ is minimized such that the worst-case approximation over all ECG signals is above a certain threshold.

ANSI/AAMI EC13 test waveforms are used to present an empirical proof of our concept [42]. In the experiments, the amount of representative data required for a target level of approximation accuracy is minimized, and results for ECG signals of length $N = 4096$ derived from the aforementioned test waveforms are presented. In particular, the intuition that the proposed hybrid approach performs better signal approximation compared to pure Fourier as well as pure wavelet strategies is corroborated through these experiments. In this regard, the signal *aami3c*, found to be the least com-

pressible, and therefore is of particular interest. Indeed the other waveforms, while more compressible, exhibit similar trend.

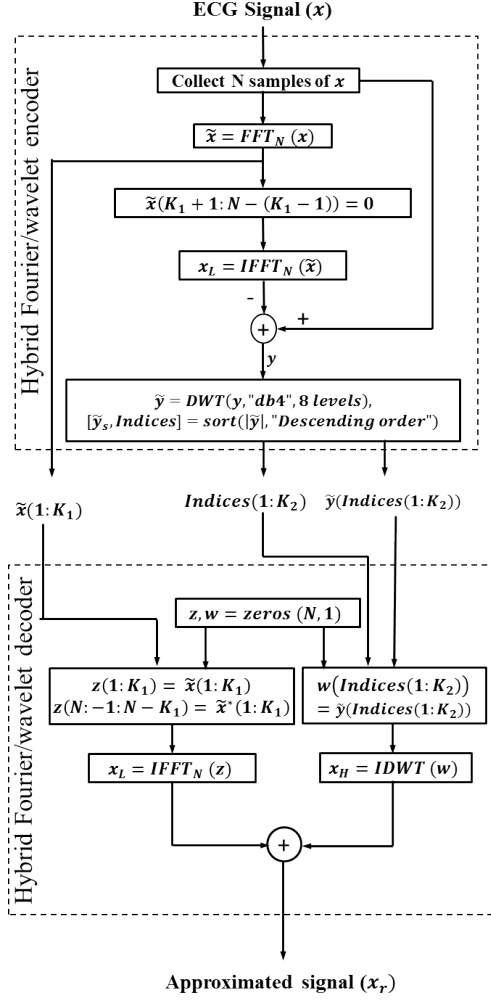


Figure 2.6: Flow chart for the proposed hybrid Fourier/wavelet encoder and decoder.

Continuing with figure 2.6, outputs from the encoder are fed to the decoding algorithm, which performs the following operations: (1) A new vector z is formed where the preserved K_1 low-pass Fourier coefficients are restored, the last $K_1 - 1$ coefficients are populated by the time-reversed conjugated version of preserved coefficients (while dropping the dc coefficient), and the rest of the entries are set

In particular, following savings are obtained in encoded data volume in hybrid approach over the pure wavelet method: 4.15%, 6.71% and 7.81% corresponding to respective accuracy level 99%, 98% and 97%. More dramatic savings are obtained, when comparison is made to the pure Fourier method. Further, pure Fourier analysis accumulates error near temporal feature points, which manifests as large dynamic range of error and high peaks in windowed error variance. Pure wavelet analysis, on the other hand, distributes the error more evenly, thereby reducing the error dynamic range as well as the height of peaks in windowed error variance. Interestingly, while saving on the number of required coefficients, our hybrid approach retains the desirable error shaping observed in the pure wavelet technique.

2.4.1 Proposed Algorithm

The proposed algorithm for encoding and decoding is depicted in figure 2.6, and detailed below. While encoding, first N samples of the ECG signal x are collected, and its N -point FFT \tilde{x} is obtained. The first K_1 Fourier coefficients (while preserving both the real and the imaginary parts) are assigned to the first output of the encoder. Continuing, a new coefficient vector comprised of the first K_1 and the last $K_1 - 1$ Fourier coefficients is created, and the rest of the coefficients are set to zero. Next the N -point Inverse FFT (IFFT) of the above vector produces the low-pass component x_L , which is in turn subtracted from the originally collected samples of x . The difference signal, the high-pass component y , is transformed using N -point discrete wavelet transform (DWT) to \tilde{y} , and the K_2 most significant coefficients of \tilde{y} are identified. The locations and values of those significant coefficients constitute the second and the third outputs of the encoder, respectively. Note that the algorithm inputs N samples of signal x , and outputs $2(K_1 + K_2)$ representative numbers (consisting of transform coefficients and some of their locations), and leads to a compression ratio of $\frac{N}{2(K_1 + K_2)}$. In these experiments, N is fixed, and (K_1, K_2) is optimized subject to a target approximation accuracy.

to zero. Then the N -point IFFT of the above vector z is taken to obtain an approximation x_L to the low-pass component. (2) A second new vector w is formed where the preserved wavelet coefficients are restored to their original locations and the rest of the entries are set to zero. The N -point IDWT of the above second vector w then produces an approximation x_H to the high-pass component. Finally, the addition to these approximated components produces the desired approximation to the original ECG signal x .

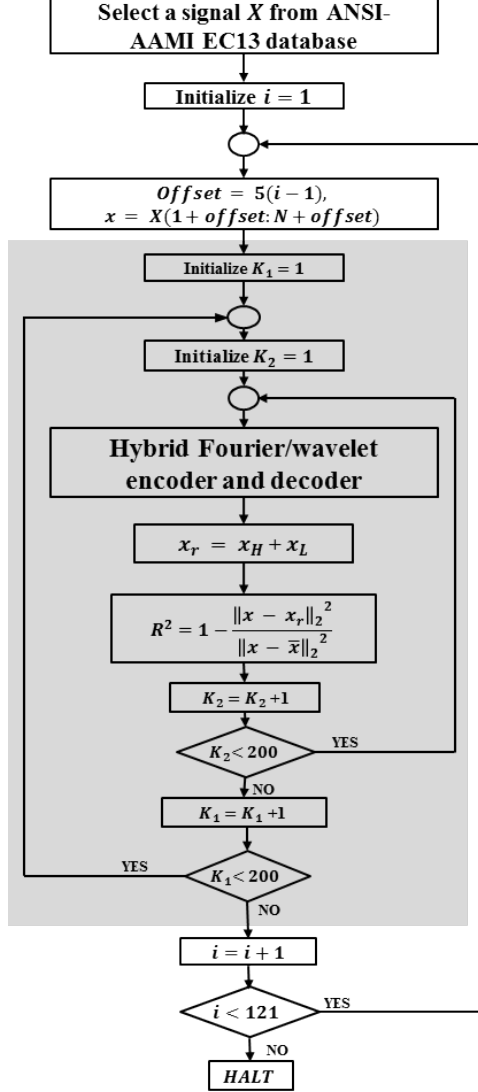


Figure 2.7: Flow chart for experimental data generation.

2.4.2 Experimental Data Generation

Now the experimental setup and procedure is described. As alluded earlier, test ECG signals from the ANSI/AAMI EC-13 dataset [42] are generated. As detailed in figure 2.7 (treat the shaded region as a single black box for the time being), from each record, windows of length $N = 4096$ (lasting approximately 5.7 seconds) are taken each at successive shifts of 5 samples (0.0069 seconds), and 121 test signals are created in the process. Here two important facts should be noted. Firstly, signal vectors encompasses multiple (usually, five or six) QRS complexes, and are meaningful for clinical purposes. Secondly, the aforementioned signal translates, despite originating from the same record, are known to exhibit highly variable behavior under wavelet transformation; such variability is also noted in section 2.4.3. Further, repeating the process for the four records at hand, altogether 484 test signals are generated.

Next the quantity $2(K_1 + K_2)$ is minimized, subject to a target signal accuracy. To this end, a test signal is picked, and the parameters K_1 and K_2 are varied from 1 to 200 in steps of 1 as depicted in the shaded region of figure 2.7, thus generating 40000 candidate approximations of the signal at hand. These numbers arise by virtue of the frequency content of the signals and change from database to database. In the concluding part of the chapter where similar experiments with Arrhythmia database are provided, the search space limits for K_1 and K_2 are different. The above process is repeated

for each of the 484 test signals (121 snippets for each of the four signals). Having generated these data, only those (K_1, K_2) pairs, for which the approximation accuracy is above the preset threshold for each of the 484 test signals are retained. From the retained ones, that (those) (K_1, K_2) pair(s) is(are) picked, for which $2(K_1 + K_2)$ takes the least value. To avoid confusion, instead of K_1 and K_2 ,

	99% R^2 score	98% R^2 score	97% R^2 score
Fourier data volume	410	352	312
Wavelet data volume	386	298	256
Fourier+Wavelet=Total volume(Hybrid)	170+200=370	166+112=278	168+68=236
% savings over wavelet approach	4.15	6.71	7.81
% savings over Fourier approach	9.75	21.02	24.36

Figure 2.8: Optimization of encoded data volumes for *ami3c* subject to target R^2 scores.

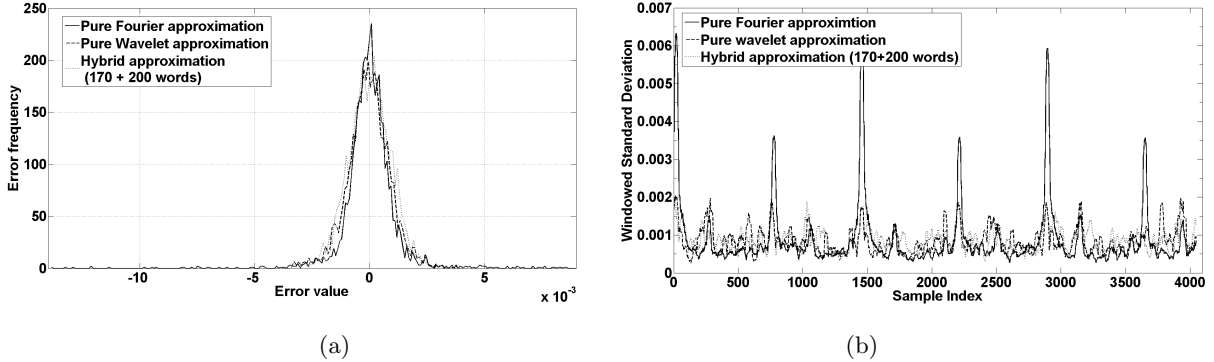


Figure 2.9: Record *ami3c*: approximation with encoded data volume 370 words, (a) Error distribution for target accuracy 99%, (b) Windowed error variance with window size = 16.

in tables and plots, $2K_1$ and $2K_2$ are shown, which are the respective encoded data volumes corresponding to Fourier and wavelet analyses, so that their sum gives the total volume of the encoded data.

Specifically, in order to claim superiority of the proposed hybrid technique, it is necessary to not only demonstrate higher compression subject to an approximation accuracy level, but also desirable error shaping. This has been addressed next.

2.4.3 Results

The first experiment described in section 2.4.2 is presented in the beginning. In the process, it is observed that, for any pair (K_1, K_2) , the test signals derived from record *ami3c* exhibit the least approximation accuracy. Thus the record *ami3c* is identified as the least compressible among the records at hand. Specifically, figure 2.8(a) shows the Fourier data volume $2K_1$ versus the wavelet data volume $2K_2$ such that the corresponding pair (K_1, K_2) meets the target accuracy level, set at 99%, 98% and 97% in three related experiments. Note that $K_2 = 0$ corresponds to a pure Fourier strategy, whereas $K_1 = 0$ corresponds to a pure wavelet strategy. Interestingly, a hybrid Fourier/wavelet strategy achieves the minimum encoded data volume. The specific “Fourier+wavelet=total” data volume figures for the respective accuracy levels are given in figure 2.8(b), and are compared against the pure strategies. Substantial savings are seen over the pure wavelet strategy, and even more dramatic savings over pure Fourier strategy.

Fig. 2.10 shows few examples of signal approximation for a sample of *ami3c*. The waveforms 2.10(b), 2.10(d), 2.10(f) and 2.10(h) are signal approximations. The corresponding errors are displayed immediately below each waveform. The histograms of errors for these cases are shown in

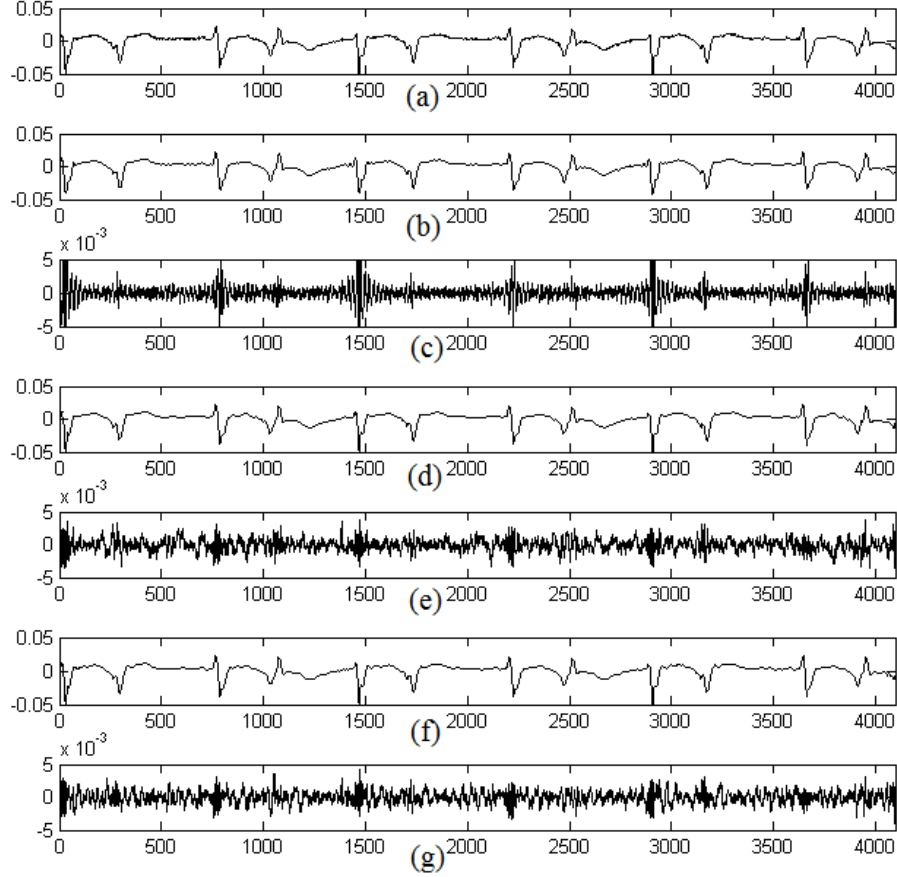


Figure 2.10: Signal approximation of *aami3c* record with encoded data volume of 370 words: (a) Original signal, (b) Fourier coefficients, (d) Wavelet coefficients, (f) 170 Fourier and 200 wavelet coefficients; corresponding R^2 scores: (b) 0.9791, (d) 0.9893 and (f) 0.9907; waveform (c), (e) and (g) are errors in (b), (d) and (f).

figure 2.9(B). The total number of coefficients chosen is 185 in each case because it was the minimum number required (best worst-case) to achieve 99% R^2 score for *aami3c* with hybrid approach (Fig. 2.9 (A)). It is observed that *aami3c* is the critical signal as it requires more number of coefficients to achieve approximation with a certain fidelity by virtue of its sharp variations in time. In other words, *aami3c* is least compressible among the signals in ANSI/AAMI EC-13 database and one can tune and test the algorithms for *aami3c*. The results shown in Fig. 2.10 are best worst-case performances over all 484 snippets. Same experiments were done on the other signals, namely *aami3a*, *aami3b* and *aami3d*, and results obtained were even better. This indicates that Hybrid approach outperforms Fourier and wavelet approximation schemes.

As reasoned earlier, error characteristics are analyzed next. As depicted in figure 2.9(a), the error distribution for Fourier approximation admits large errors with significant probability. The wavelet and hybrid approximation errors turn out less significant. Not surprisingly, the former has a variance 15.8×10^{-7} , whereas the latter two have virtually indistinguishable error variances at 8.61×10^{-7} and 8.67×10^{-7} , respectively. Taking a closer look, in figure 2.9(a) the windowed error variance is plotted, where the Fourier technique exhibits high peaks, whereas the wavelet and the

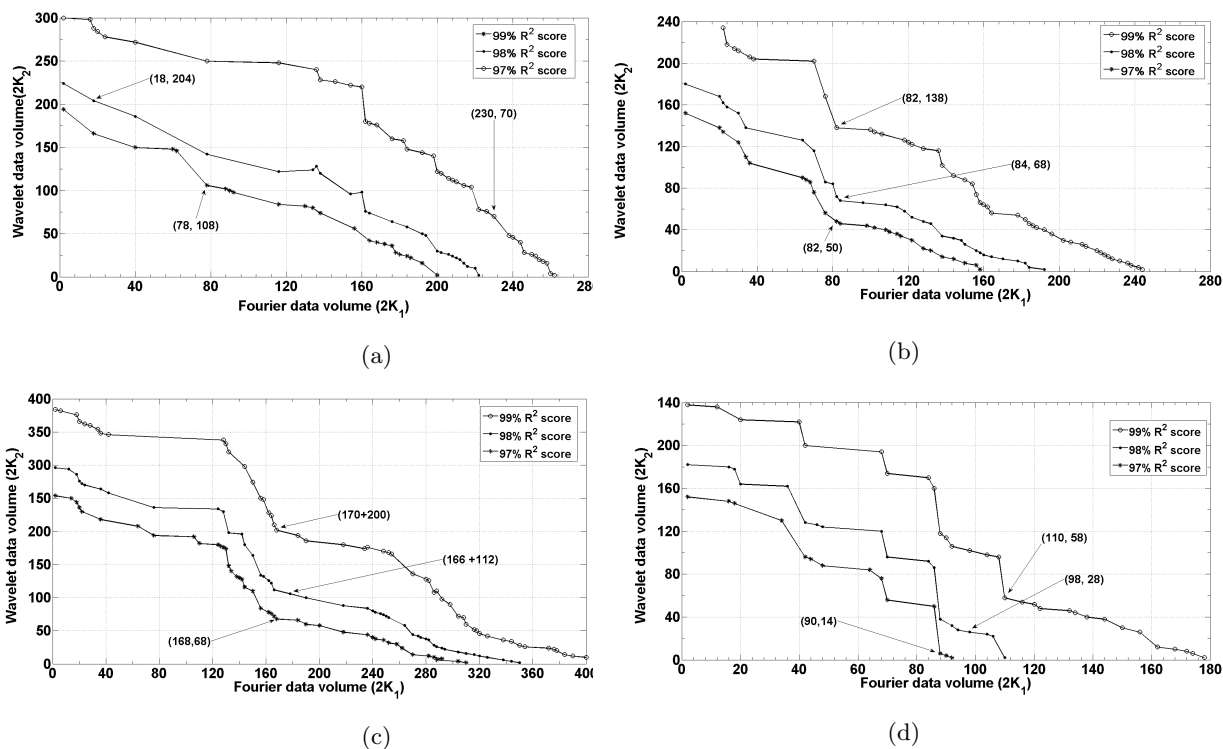


Figure 2.11: Number of components to achieve particular approximation accuracy: (a) *aami3a*, (b) *aami3b*, (c) *aami3c* and (d) *aami3d*.

hybrid schemes distribute the error almost indistinguishably.

Next the same signal approximation problem is posed from a slightly different angle. In particular, the encoded data volume is fixed at 370 words, and signal reconstruction and error characteristics are compared under pure and hybrid strategies. Figure 2.10 depicts the original signal, rival approximated signals, and the corresponding error waveforms. Again, the Fourier analysis appears to lump significant error at feature points, whereas the wavelet and hybrid strategies, which are virtually indistinguishable, appear to spread the error more evenly. In summary, hybrid strategy proves to be more efficient than the state-of-the-art pure wavelet-based technique, without sacrificing the desirable error characteristics. Of course, this strategy provides more dramatic savings over pure Fourier strategies. Finally, it is observed that the general behavior of test signals generated from record *aami3c* is exhibited by those generated from the other records. This is demonstrated for the record *aami3b* in figure 2.11. Note that a smaller encoded data volume now suffices to meet the same accuracy level, when compared to figure 2.8(a) for *aami3c*.

2.5 Comparison of Hybrid Approximation Method with other Representation Methods

In this concluding section, the proposed hybrid approximation technique is finally compared with well known transform based representation methods. ECG signals from MIT-BIH Arrhythmia Database have been used (see Table 1.1). The primary reasons for choosing this dataset include: (i) wide

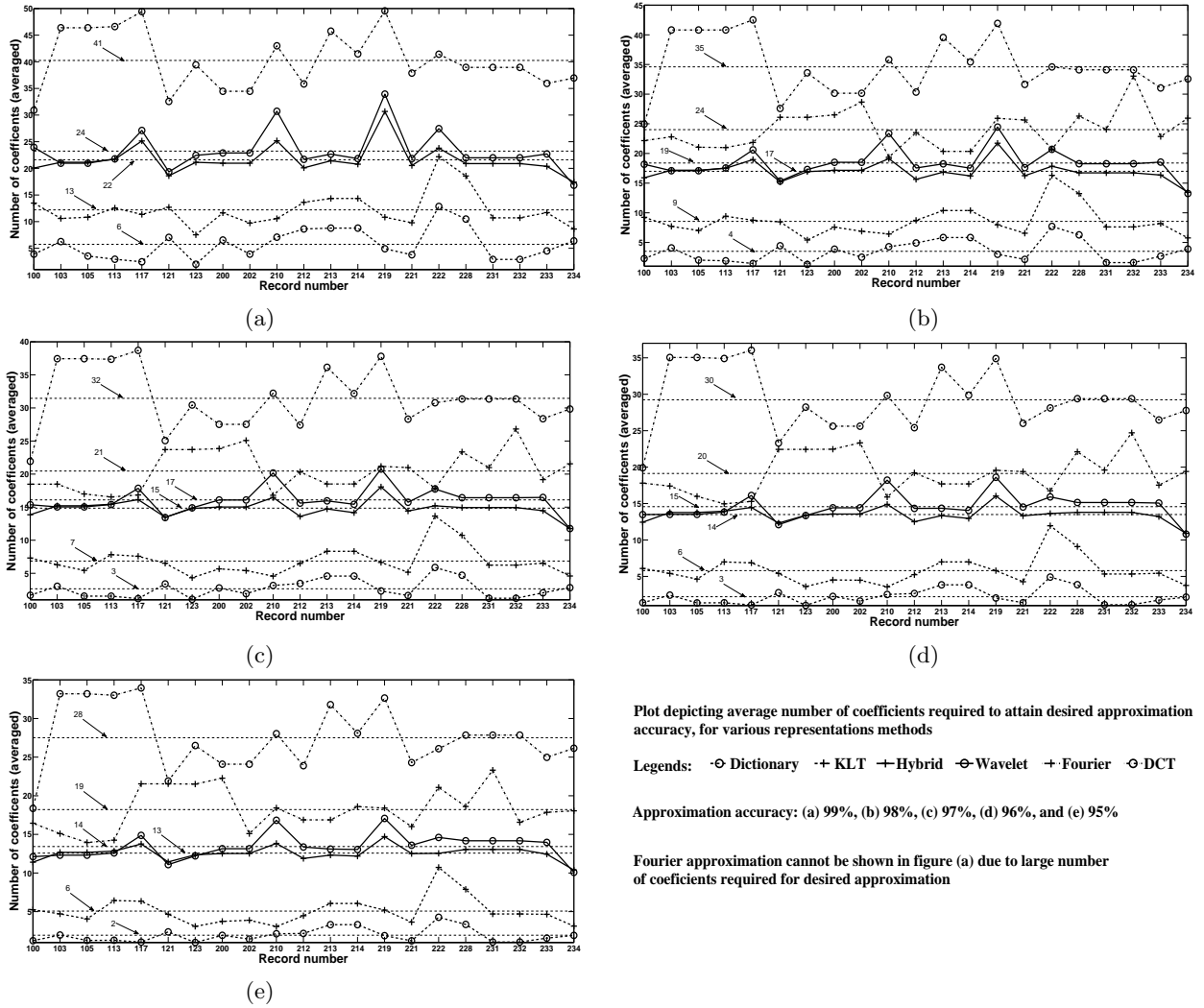


Figure 2.12: ECG signal approximation for Arrhythmia Database

popularity across the literature, (ii) availability of annotations, making it easy to align the ECG features in a snippet chosen, which necessary for training purposes in case of KLT and dictionary based approximations, and (iii) variety of disease classes available. Length of a signal snippet was chosen to be 256 samples. Thus, for example, for a record number 100 from Arrhythmia database, all possible segments of length 256 samples were considered. Annotations provided in the database were used to ensure that R-peak appears in the center of a signal snippet. These snippets were then tested for cumulative energy compaction using various wavelets and also with hybrid approximation method, described earlier. Additionally, energy packing by DCT and FFT coefficients was also studied. In case of representation in KL-basis as well as dictionary, entire dataset was divided into two parts. One of those was taken as training data and the other was taken as testing data (see [51, 52] for more details). The procedure for cumulative energy packing by coefficients of KL representation is same as that for projection on any orthogonal basis. However, in case of dictionary based representation, one has to train an overcomplete dictionary and solve sparse recovery problem. We describe the sparse recovery problem in greater details in the next chapter.

Figure 2.12 depicts average number of coefficients required for targeted approximation accuracy. The horizontal dotted lines show average number of coefficients, rounded to nearest integer greater than the actual average. All the subsequent calculations reported here are according to these rounded values. One immediate observation here is that Fourier representation requires very large number of coefficients for energy compaction, on account of sharp features in the ECG. Therefore, results corresponding to Fourier approximation do not appear in the plot showing results for 99% target accuracy (R^2 score). Overcomplete dictionary based representation is the most succinct, closely followed by KL approximation. The proposed hybrid methodology outperforms wavelet and DCT based representation. Although one may argue that the advantage of hybrid method over wavelet representation is not significant, it is important to note that as opposed to the results shown for signal of length 256 samples, the total savings in terms coefficients for the entire signal amounts to a larger quantity. Nevertheless, one can observe the percentage savings in terms of coefficients, for hybrid method over wavelet representation, which are 8.33%, 10.5%, 11.8%, 6.66% and 7.14%, for targeted accuracy of 99%, 98%, 97%, 96% and 95%, respectively.

Further, one should note that the length of the signal samples was chosen to be 256 samples and R-peaks were centered in such signals, to facilitate the training procedure for dictionary and KL-basis. Thus, significant computational resources are demanded by these two methods. Although overcomplete dictionary offers sparsest representation, it does may not fit into proposed low cost framework, mainly due to training procedures. Even if one fixes a dictionary, one has to store a large number of atoms. In the study presented here, size of the dictionary was chosen to be 256×1000 , requiring storage of 1000 atoms. On account of wide variety of ECG signals, it may be necessary to repeat the training procedure. In contrast, fixed bases such as Fourier, wavelet and thus hybrid method remain attractive due to simple procedures to generate this bases.

Chapter 3

Low-rate Sampling of ECG Signals

This chapter discusses low rate sampling of ECG signals, which is possible due of sparsity of ECG signals in wavelet bases. A brief overview of sampling theory is provided in section A.1. The universal nonuniform sampling method mentioned here relies on recent advances in compressive sampling theory which is briefed in section A.3. In the beginning, compressive sampling of ECG signals with randomized measurements is presented. The recovery algorithms proposed is called targeted orthogonal matching pursuit which is explained in section 3.1.1. Next, use of CS measurement matrices that are row restrictions of identity matrices is presented. The method is termed as universal because its recovery performance remains consistent irrespective of the sampling locations.

In the beginning, the problem setup is described as follows. A typical ECG signal has significant frequency components well beyond 125Hz, and a sampling frequency of greater than 500Hz has been prescribed for faithful reconstruction [38]. Indeed, professional-grade equipments use sampling rates of 500Hz, 720Hz and 1000Hz [42, 2]. Such high rates corresponding to uniform sampling are not attractive for our envisages of low-power operations. Against this backdrop, one would naturally ask: Can the average sampling rate (and hence the power requirement) be significantly reduced is nonuniform sampling is adopted? What will be the opportunities and obstacles facing a low-rate nonuniform sampling scheme? This work attempts to answer some of these questions with special emphasis on universality.

If one samples uniformly at a frequency $f_s \geq 2f_{max}$ (where f_{max} denotes the maximum significant frequency in the signal), then one is guaranteed an accurate reconstruction via sinc interpolation functions by the Nyquist theorem [53]. Further, uniform sampling at rate f_s still suffices even if the signal undergoes a temporal shift, because such shift does not alter the magnitude of the Fourier spectrum. Clearly, any signal satisfying $f_s \geq 2f_{max}$ or its translates can be uniformly sampled without loss. In other words, a uniform sampling is universal for all signals satisfying the Nyquist theorem. Unfortunately, similar universality properties do not hold for nonuniform sampling in general. Specifically, a general criterion for faithful reconstruction from nonuniform sampling, analogous to the one mentioned above for uniform sampling, is yet to be discovered. To further complicate matters, even if a signal ensures faithful reconstruction from nonuniform samples taken in a particular pattern, translates of that signal may not admit the same even if sampling patterns are unchanged. In this work, empirical universality of nonuniform sampling patterns for ECG signals is explored.

Specifically, noting that ECG signals admit sparse representation in certain orthogonal bases such as Daubechies Wavelet ‘DB4’ [26], and using the compressive sampling (CS) formalism [54], Orthogonal Matching Pursuit (OMP) to reconstruct the signal from nonuniformly sampled data [55, 56] appears to be suitable recovery method. Note that any nonuniform sampling pattern does not guarantee faithful reconstruction; rather, a pattern (alternatively known as a measurement matrix) is required to satisfy a restricted isometry property (RIP, see (A.10)). As a first step, this work demonstrates a proof-of-concept using ANSI/AAMI standard ECG waveforms sampled at 720 Hz, and their temporal translates [42]. In the course, it is observed that significant wavelet coefficients occur within certain range of locations, which leads to a parameterized Targetted Orthogonal Matching Pursuit (TOMP) algorithm for ECG signals. Finally, it is shown that universal nonuniform sampling at an average rate of 144 Hz (well below 500 Hz, suggested in literature [38] can be realized with specific performance guarantee.

3.1 Compressive Sampling of ECG Signals

Compressive sensing (CS) theory asserts that one can recover a signal from a few linear non-adaptive measurement, far fewer than those guided by Nyquist rate, if the underlying signal admits sparsity in some sense and the measurement process preserves the isometry within certain bounds [54]. CS theory has been explained briefly in section A.3. As alluded earlier, CS based applications depend on three key factors, namely, the measurement operator, signal sparsity and recovery scheme. In chapter 2, wavelets that offer sparse representation were identified. In this chapter, the remaining two factors namely measurement matrix and recovery scheme have been discussed with emphasis on universality. The recovery scheme adopted is based on Orthogonal Matching Pursuit (see section A.3.2). The OMP algorithm is modified to what is called as Targetted Orthogonal Matching Pursuit, explained next.

3.1.1 Targetted OMP (TOMP)

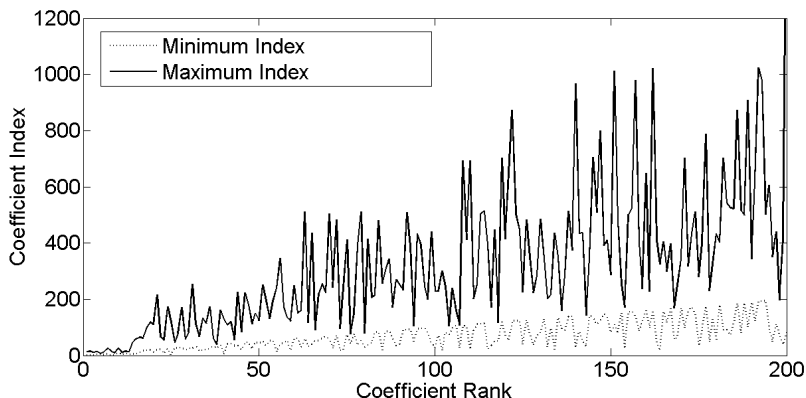


Figure 3.1: Range of coefficient indices occupying ranks 1–200.

Given the measured vector y and the measurement matrix Φ , one finds the coefficient of x with the largest magnitude by projecting \tilde{x} onto each column of A and selecting the largest $\langle \tilde{x}, a_j \rangle$,

Input: Measurement matrix: $\Theta = \Psi\Phi$ where $\Theta \in \mathcal{R}^{M \times N}$, measurement vector: $y \in \mathcal{R}^M$, Set of column indices for i^{th} stage: C_i where $C_{i-1} \subseteq C_i$, Set of stagewise iteration limits I_i , $\#max_number_of_stages$, Set of thresholds P_i

Output: Recovered signal: \hat{x} , support set: $S \subset [1, N]$

Initialization: $S = \emptyset$, $flag = 0$, $\#iterations = 0$ Residue: $res = y$;

while *number of stages* $i \leq \#max_number_of_stages$ **OR** $\|res\|_2^2 \geq \epsilon$ **do**

while $flag == 0$ **do**

Sweep: $u = \Theta^T|_{C_1} res$;

Update support: $j_0 = \text{index of max } |u|$, $S = S \cup j_0 \quad \forall j_0 \notin S$;

Update provisional solution: $\hat{x} = \arg \min \|y - \Theta|_{C_1} x\|_2$ subject to support set S ;

Update residue: $res = y - \Theta|_{C_1} \hat{x}$;

if $\|\hat{x}\|_2^2 \geq P_1\% \|y\|_2^2$ **OR** $\#iterations \geq I_1$ **then**

$flag = 1$;

end

end

end

Algorithm 1: Targeted Orthogonal Matching Pursuit (TOMP) Algorithm

where a_j is the j th column of A . Once such coefficient is identified, a least-squares problem is solved assuming it is the only non-zero coefficient. The new estimate for \hat{x} is used to compute the estimated signal x . The algorithm is iterated using the residual to solve for the next largest coefficient of \hat{x} one at a time. By iterating k times, one finds an k -sparse approximation of the transform domain vector.

Here OMP algorithm is modified to target it for standard ECG signals [42]. First discrete wavelet transform of signal using Daubechies ‘DB4’ basis is calculated. The coefficients are arranged in the decreasing order of magnitude, and ranked. It is noticed that the sorting indices that occupy a certain rank for the signals under consideration lie within a certain range. This observation is depicted in figure 3.1.

In view of figure 3.1, the OMP is targeted in the following manner. Originally, one selects a new index from the entire search space of indices. In contrast, the search space is restricted according to the rank of the said index. Specifically, the coefficient ranks are divided into certain stages, and different search space is used for each stage. However, the stage is dictated also by the cumulative energy so far recovered. Each coefficient index is added to the support, and the coefficient value is reconstructed exactly as in OMP. However, the stage r is parameterized by three numbers: C_r indicates the maximum index location to be searched, P_r the maximum cumulative energy to reach to go to the next stage, and I_r the maximum number of iterations to complete before going to next stage. One moves on to stage $r + 1$ if either the energy reaches P_r , or the number of iterations reaches I_r . Over several runs, a five stage implementation was adopted, with parameters: $C_1 = 100$, $C_2 = 200$, $C_3 = 500$, $C_4 = 1000$, $C_5 = 1500$, $P_1 = 95\%$, $P_2 = 97\%$, $P_3 = 98\%$, $P_4 = 99\%$, $P_5 = 100\%$, $I_1 = 80$, $I_2 = 80$, $I_3 = 90$, $I_4 = 40$, $I_5 = 40$.

3.1.2 Compressive Sampling of ECG Signals using Random Measurement Matrices

This section presents greedy recovery of ECG signals from the incomplete measurements. The measurement matrix Φ is chosen to be sparse random matrix whose entries are sampled from normal

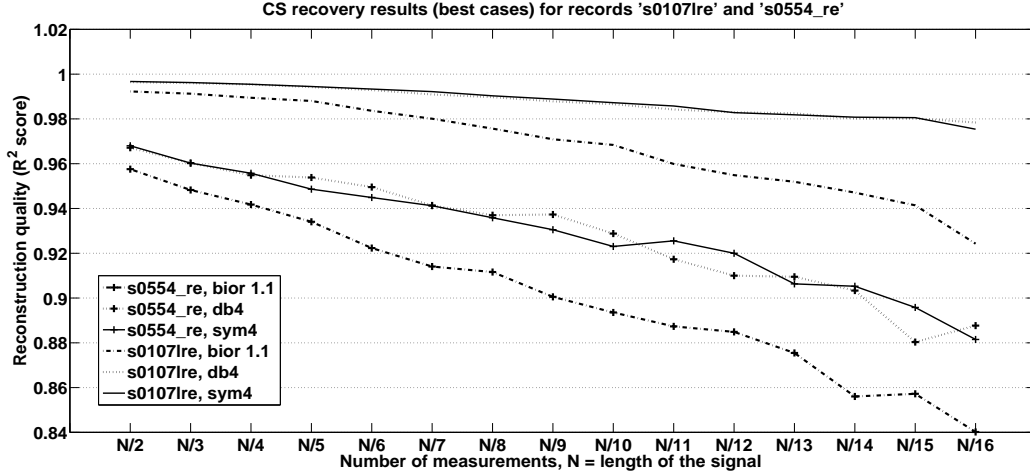


Figure 3.2: Signal recovery from randomly chosen samples

distribution. Such matrices are known to satisfy RIP with very high probability. The matrix Φ is $m \times N$, where $m = N/d$ (rounded to integer) and $d = 2, 3, \dots, 16$. For each m , 1000 random matrices were obtained and TOMP was employed to solve the CS recovery problem in each such case.

As an illustration, two signal records, namely ‘s0107lre’ (highly compressible) and ‘s0554_re’ (less compressible), from PTB dataset, have been chosen. Notice that the ‘sym4’ basis leads to the best R^2 reconstruction from the same number of measurements, closely followed by ‘db4’, and distantly followed by ‘bior1.1’. This observation corroborates the findings from figure 2.4.

3.2 Universal Nonuniform Sampling Scheme for ECG

Although compressive sensing followed by greedy recovery is able to offer faithful reconstruction subject to target R^2 score, it is costly from hardware perspective. This is because the measurement matrix is chosen to be random Gaussian sensing matrix and requires multiplication operation. A low power alternative to this is achieved by choosing measurement matrices that do not need multiplication. Towards this, two empirical studies have been presented.

- Row restrictions of identity matrices. Indices of the rows to be kept come from random permutations.
- Row restrictions of identity matrices. Instead of completely random restrictions, we chose random indices in uniform bins. For example, if one wants to keep a fraction $1/d$ of total samples randomly, one chooses a number from every non overlapping consecutive partitions of length d in $[1, N]$, where N is the number of rows.

In each of the case 100 candidate patterns were generated and the $P0$ problem was solved in each case. The following part explains use of first type of matrices. Partial results with second type of matrices are presented in the end of this chapter. If $A1$ is set of all the matrices of first kind and $A2$ is set of all the matrices of second kind, then one can write $A1 \subseteq A2$. Uniform downsampling of the already sampled signals, which uniform restriction of identity matrix, can be seen as subset of $A2$.

Four signals from the ANSI/AAMI standard for testing ECG devices [42] were considered. Those have been empirically found to exhibit in certain sense the extremes of ECG signals. Since the goal is to restrict to a manageable set of signals, yet be able to demonstrate universality, those signals appear to be a natural choice.

3.2.1 Experiments

This empirical study considered windows of 4096 samples from each original signal (which amounts to 5.7 seconds worth of data), and obtained 121 such windows each shifted by 5 samples (0.0069 seconds), producing 121 translates for each waveform, i.e., 484 snippets. At the same time, 100 downsampling patterns for each of average downsampling ratios 2, 3, 4, 5, 6 were generated. Further, each of the down sampling pattern is used for all 484 snippets for the corresponding downsampling factor (2, 3, 4, 5, 6). Although inadequate for clinical purposes, R^2 statistics, defined in (1.1) is used for quality of signal reconstruction as the design criterion for comparing between various patterns [2]. Specifically, the worst performance of each pattern is taken, and the pattern that produces the best among such worst performances is picked. In other words, the pattern that guarantees the best worst-case performance is chosen. However, such worst-case design might be too conservative. Therefore, best lower 5-percentile, 10-percentile, and 20-percentile performances as well are considered.

3.2.2 Results

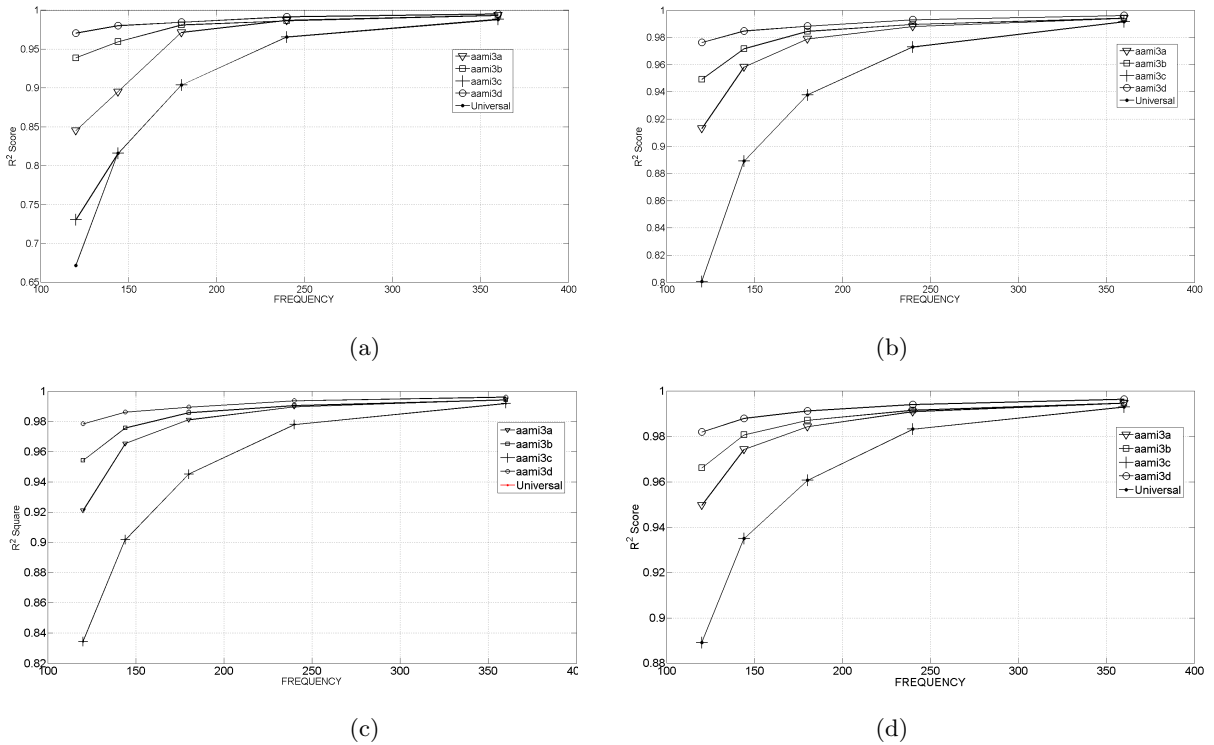


Figure 3.3: Best R^2 statistics over all patterns for average downsampling 2, 3, 4, 5, 6 for each individual signal as well as over all signals: (a) 0 percentile, (b) 5 percentile, (c) 10 percentile and (d) 20 percentile.

The best worst-case (lower zero percentile) performances are plotted in figure 3.3a. Similarly, The best lower 20-percentile performance are plotted in figure 3.3d. In each figure, such performances are plotted for each individual signals, as well as over all signals. Note that downsampling by 2, 3, 4, 5, 6 correspond to respective average sampling rates of 360, 240, 180, 144, 120 Hz, respectively. From the above, four inferences are drawn:

1. Performance degrades with lower average sampling rate, as expected.
2. The desired performance corresponding to a lower percentile is lower, as expected.
3. Best 20-percentile performance over all signals and that for “aami3c” are identical.
4. Best worst-case performance over all signals and that for “aami3c” are identical for all down-sampling factors except 6.

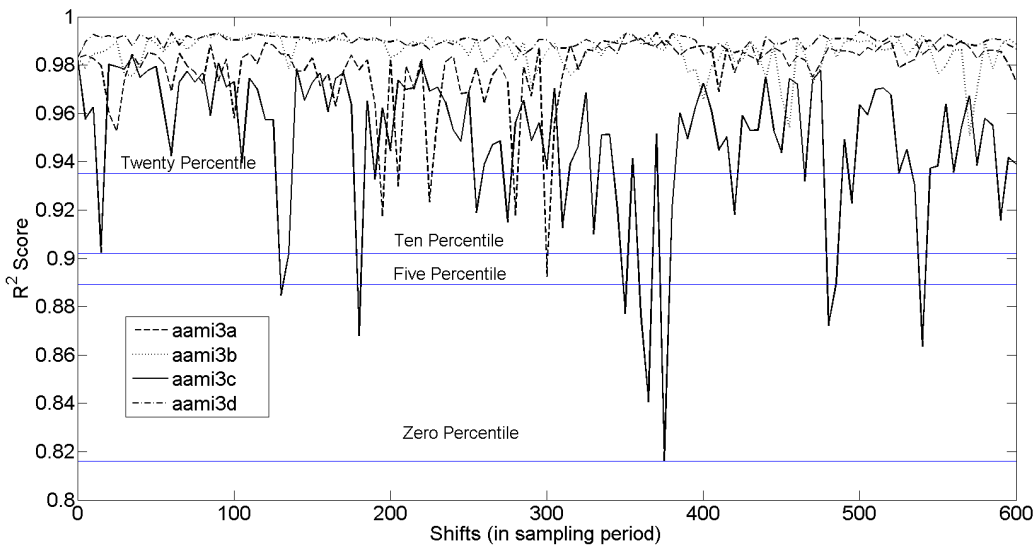


Figure 3.4: Performance variation of the optimal pattern at average sampling rate of 144 Hz with temporal shifts (translations).

Based on this, one should adopt “aami3c” as the critical signal for which a proposed system need testing. However, most importantly, an average sampling rate of 144 Hz appears adequate for all signals except one critical one, for which too it is adequate 80% of the time. In other words, near-universality of a sampling pattern operating at an average rate of 144 Hz is demonstrated.

Next, the performance variation of the optimal pattern for a representative downsampling factor of 5 (corresponding average sampling rate is 144 Hz) for different temporal translates is observed. Not surprisingly (in view of figures 3.3a and 3.3d), the same pattern achieves best worst-case, 5-percentile, 10-percentile, and 20-percentile performances over all signals. In particular, figure 3.4 shows that the same sampling pattern behaves very differently for different temporal translates. Further, performance index and the percentile varies in a complex manner. The performance difference is 0.073 for moving from 0-percentile to 5-percentile, 0.0126 for moving from 5-percentile to 10-percentile, and 0.033 for moving from 10-percentile to 20-percentile, indicating a non-monotone behavior.

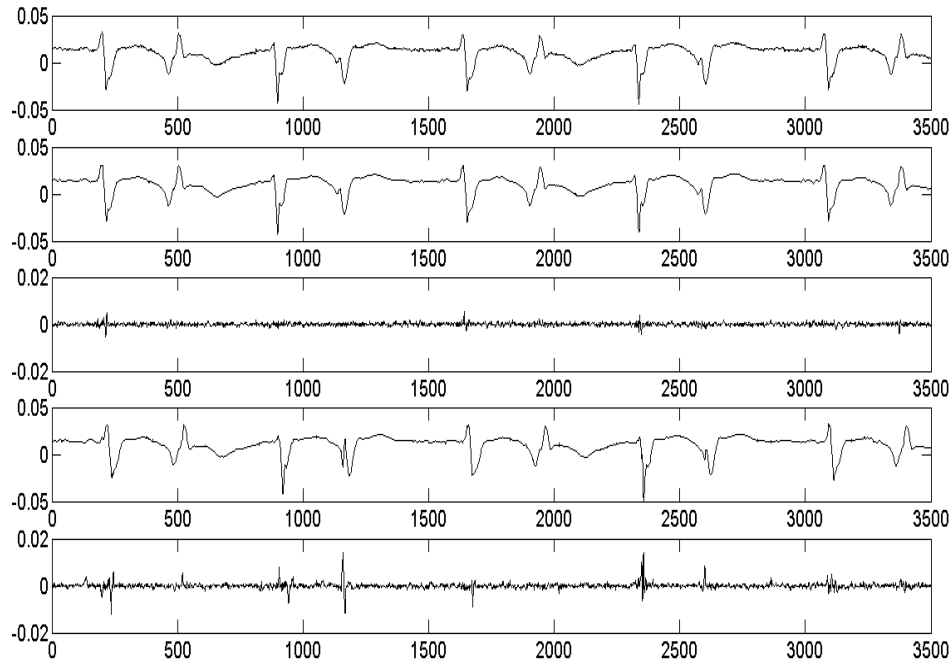


Figure 3.5: Reconstructed Signal after down-sampling by 2, R^2 Score = 0.996 and down-sampling by 5, R^2 Score = 0.984.

Finally, the best worst-case performances are quite conservative. For example, although the best worst-case performance at average sampling rate of 360 Hz and 144 Hz are 0.983 and 0.815, respectively (both achieved for “aami3c”), one can achieve performances of 0.996 and 0.984 with same patterns with favorable translations. In summary, we have demonstrated a faithful nonuniform sampling scheme at a low (sub-Nyquist, as ECG signals generally contains frequency components above 100 Hz [38]) average rate which is nearly universal.

In conclusion, it should be noted that the here goal has been to minimize the average sampling rate, and the proposed nonuniform sampling scheme takes a step towards it. Recall that the primary motivation stems from low-power operation of the sampling unit (ignoring discretization of signal magnitude for simplicity). Although proposed scheme provides compression, optimizing it has not been the focus. For compression schemes for ECG signals, see [36, 35, 25]. For theoretical limits of compression, see [57]. In closing, note that the number of nonuniform sampling patterns is very large. In fact, for signal length $n = 4096$, the number of possibility is an extremely large number with over 2000 decimal digits. Admittedly, most of those patterns are of little value for nonuniform sampling, but the number of “good” patterns are still much larger than 100. Since only 100 nonuniform sampling patterns were generated at random in this work, it is likely that patterns giving better reconstruction performance than the present proof of concept will be discovered.

Finally, non-uniform sampling with second type of matrices is presented here. This exercise is performed on Arrhythmia database, as the sampling rate during recording was very low (360Hz), providing another extreme testing condition for the proposed method. MIT-BIH Arrhythmia database, recorded at 360Hz, has 48 signals. Snippet size was taken to be 4096 samples with an overlap of

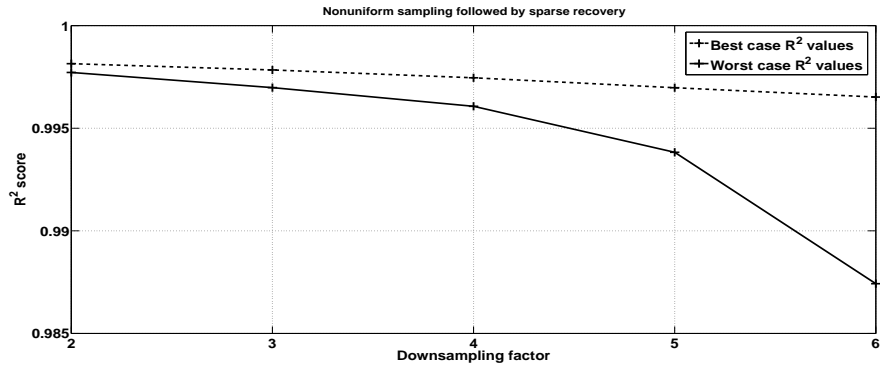


Figure 3.6: Signal recovery from randomly chosen samples

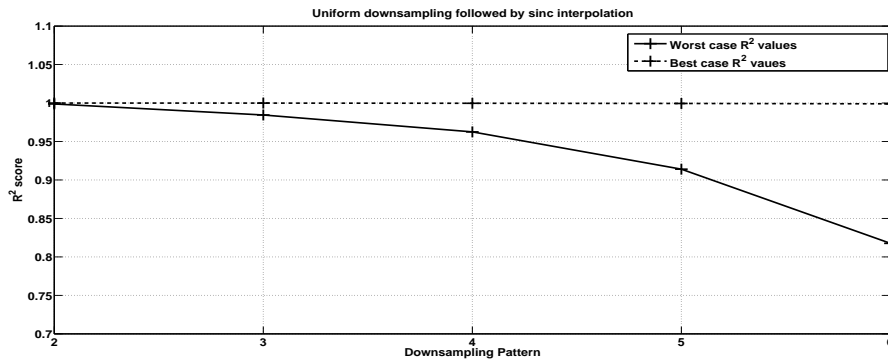


Figure 3.7: Uniform downsampling and sinc interpolation

2048 samples between two snippets. Results available for 4 signals at present are presented. Figure 3.6 shows best and worst case performances for downsampling rates of 2, 3, 4, 5 and 6. Note that best case performance for uniform downsampling followed by sinc interpolation always outperforms nonuniform sampling followed by greedy recovery. However, in the worst case scenario, the nonuniform sampling is seen to perform better. All the results shown here are averaged over several signals.

Chapter 4

Summary and Discussion

The two main focus areas of this work, described in section 1.1 are (i) minimal linear representation of electrocardiogram signals, which enables one to achieve (ii) low rate sampling of electrocardiogram signals. The thesis reports findings on choice of wavelet basis for sparsest representation, a hybrid Fourier/ wavelet method for even sparser representation and an universal non-uniform sampling scheme for ECG signals followed by sparse recovery. On account of wide variety of ECG signals and thereby inability to propose model(s) for ECG signals, the work takes help of several empirical studies to provide proof of concepts and support the claims made. In the course of these studies, several interesting insights were obtained. This chapter discusses limitations and future scope in this direction.

4.1 Sparse Representation

Chapter 2 has presented an empirical study on cumulative energy packing by wavelet coefficients. It was observed that ‘sym4’ and ‘db4’ wavelets offer highly sparse representation. This study was carried out on PTB database. Further, hybrid approximation method was presented which outperforms wavelets representation on average. This was demonstrated with all three databases listed in table 1.1. However, a few cases have been observed where mere Fourier or wavelet representation suffices to offer a sparse representation. In this backdrop, it is necessary to study wavelet sub band structure more closely and possibly seek for a way to switch between pure wavelet and hybrid methods. Nevertheless, hybrid approximation provides a new way to represent ECG succinctly, with desired error shaping. The next step is to test it rigorously and more importantly, extend it to a compression algorithm. An immediate idea is to perform predictive coding on low frequency part as it is mostly periodic and encode remaining part with entropy coding.

On a different note, it has been shown that hybrid method seeks a (K_1, K_2) pair based on search over all such pairs, where search limit is decided a priori. Ideally, one would attempt to separate periodic part completely and then encode the remaining localized features. In such case harmonic analysis of ECG signals shall be attempted. Speech processing community can provide some clues where voiced and unvoiced parts of a speech signal are separated. Feasibility of such approach would also be evaluated.

4.2 Reduction in Sampling Rates

With the sparse representation available, the thesis focuses on low rate sampling of ECG signals, aided by recent advances in compressive sampling theory. From the empirical studies, it appears that ECG acquisition rates well below standard rates are possible and the reconstructed signals are nearly of same quality as those obtained with standard rates. R^2 statistics supports this claim, which is a widely accepted measure for this purpose. Thus, it can be said that CS transfers the computational burden from encoder to decoder, enabling for simpler and low power implementation of encoder. An important point to be noted is that compressive sampling is believed to be advantageous over uniform sampling in terms of said savings in power consumed during acquisition. This achieved at the cost of generation of random sampling matrices at the encoder side, making it non-deployable for real time monitoring. Generation of the random matrix was eliminated by employing measurement matrices which are restrictions of identity matrices. These selected matrices were able to capture most of the information from signals. It has not been understood why these matrices are able to offer better performance whose RIP compliance is not guaranteed. One reason could be the periodicity and smoothness of ECG signals. This is planned to be explored further. An ongoing study was also reported which considers use of deterministic construction of CS matrices. Further the signal structure itself is exploited to design robust reconstruction algorithms such as Targeted Orthogonal Matching Pursuit. This is similar to the well known model based compressed sensing proposed in [58].

Finally, in the closure, it is imperative to note that the proposed algorithms were evaluated with some objective quality measure. It is necessary to collect doctors' opinion by Mean Opinion Scores (MOS) (see, for example, [43, 44, 45, 46]).

Appendix A

Theoretical Background

This work attempts to achieve low rate sampling of ECG signals maintaining the targeted reconstruction quality. Towards this, nonuniform sampling at low average rate is one possible approach. Recent advances in Compressive Sensing (CS) theory guarantee faithful signal recovery from a few random linear measurements using various optimization schemes. One of the motivations behind CS theory is the problem of data deluge due to advancement in digital devices and thereby possible inundation of communication bandwidth and power. Rates dictated by the Shannon- Nyquist theorem impose severe challenges both on the acquisition hardware and on the subsequent storage and DSP processors. Following sections present the background and theory of CS in brief.

A.1 Sampling

In this section, the sampling theory is described briefly. Given an analog signal $x(t)$, $t \in \mathcal{R}$, one obtains samples $\{x(t_i)\}$, where $\{t_i \in \mathcal{R}\}$, $i \in \mathcal{Z}$. The perfect reconstruction condition is then

$$\exists f \text{ such that } x(t) = f(t, \{x(t_i)\}), \forall t \in \mathcal{R}. \quad (\text{A.1})$$

In general f depends on x . For example, f can be found under Mean-squared error (MSE) criterion as follows

$$f^* = \arg \min_f \lim_{T \rightarrow \infty} \frac{1}{2T} \int_{-T}^T [x(t) - f(t, \{x(t_i)\})]^2 dt. \quad (\text{A.2})$$

and

$$\hat{x}(t) = f^*(t, \{x(t_i)\}). \quad (\text{A.3})$$

Uniform sampling of a bandlimited signal $x(t)$ simply involves taking the discrete set $\{x(nT_s) : n \text{ integer}\}$, where T_s indicates the sampling period. In other words, it is a specific case of the more general nonuniform sampling $\{x(t_n)\}$, where $t_n = nT_s$. In this case, the reconstruction is achieved as follows

$$\hat{x}(t) = f(t, \{x(t_i)\}) = \sum_{i=-\infty}^{\infty} x(iT_s)g(t - iT_s). \quad (\text{A.4})$$

The interpolation function in this case is independent of the signal and is given as $f(t) = \text{sinc}(t) = \sin(\pi t)/(\pi t)$.

In general, $\{t_n\}$ can be chosen arbitrarily, and indicates a sampling pattern. For simplicity, in this thesis, it is assumed that $t_n = k_n T_s$, where k_n is an integer for every n and T_s is the underlying sampling period. In other words, this work ignores certain samples, and selects the rest from an already uniformly sampled signal. Reconstruction of the original signal from such limited number of samples (measurements) is addressed in the CS theory, where faithful reconstruction is possible if the original signal admits sparse representation and the sampling pattern (measurement matrix) satisfies restricted isometry property (RIP).

Now, let x be a discrete-time signal obtained from $x(t)$ by uniform sampling. Thus, $x \in \mathcal{R}^N$. For an orthogonal basis $\Psi = \{\psi_1, \psi_2, \dots, \psi_N\}$ for \mathcal{R}^N , x is uniquely represented as $x = \sum_{i=1}^N \alpha_i \psi_i$, where $\alpha = \Psi^T x$. In transform coding parlance, one keeps K largest α_i s and discards the remaining to obtain a K -term approximation. Initial N may be large even if K is small. The set of all N transform coefficients $\{\alpha_i\}$ must be computed even though $N - K$ of them will be discarded. The locations of the large coefficients must be encoded.

In this backdrop, compressive sensing asks following question: *Why go to so much effort to acquire all the data when most of what we get will be thrown away? Can't we just directly measure the part that won't end up being thrown away?* This issue is discussed more formally in next section.

A.2 Dimensionality Reduction Problem

Generally speaking, dimensionality reduction techniques aim to extract low-dimensional information about a signal or collection of signals from some high-dimensional ambient space. Effective techniques for processing and understanding data and information often rely on some sort of model that characterizes the expected behavior of the information. In many cases, the model conveys a notion of constrained structure or conciseness to the information; considering a data vector (or “signal”) $x \in \mathcal{R}^N$, for example, one may believe that x has “few degrees of freedom” relative to its size N .

Let $\mathcal{F} \in \mathcal{R}^N$ denote the class of signals of interest, for example, class of all ECG signals. Let $\Psi = \{\psi_1, \psi_2, \dots, \psi_N\}$ be an orthonormal basis for \mathcal{R}^N . A signal $x \in \mathcal{R}^N$ is uniquely represented as $x = \sum_{i=1}^N \alpha_i \psi_i$, where $\alpha = \Psi^T x$. Let the set $\Omega = \{1, 2, 3, \dots, N\}$, whose cardinality $|\Omega| = K$. Then K -term approximation to x is written as $\hat{x} = \sum_{i \in \Omega} \alpha_i \psi_i$. Let $\mathcal{F} = \text{span}\{\psi_i\}_{i \in \Omega}$. The linear geometry of these signal classes leads to simple, linear algorithms for dimensionality reduction. An ℓ_2 -nearest “linear approximation” to a signal $x \in \mathcal{R}^N$ can be computed via orthogonal projection onto the subspace \mathcal{F} (setting α_i to zero for $i \notin \Omega$). Also, the best K -dimensional subspace to approximate a class of signals in \mathcal{R}^N can be discovered using principal components analysis (PCA) (also known as the Karhunen-Loeve transform)

In a sparse model, every signal from the class \mathcal{F} can again be represented (either exactly or approximately) using a K -term representation from some basis Ψ , but unlike the linear case in, the relevant set Ω of basis elements may change from signal to signal. Few coefficients are required to represent any given signal and algorithms for dimensionality reduction must typically adapt to the changing locations of the significant coefficients. Thus, best K -term “nonlinear approximations” can be computed simply by thresholding the expansion coefficients α in the basis (letting Ω contain the indices of the K largest coefficients and then setting α_i to zero for $i \notin \Omega$).

No single K -dimensional subspace suffices to represent all K -sparse signals; instead the set of all sparse signals in the basis Ψ forms a nonlinear union of distinct K -dimensional subspaces in R^N .

$$\Sigma_K := \mathcal{F} = \bigcup_{\Omega=\{1,2,\dots,N\},|\Omega|=K} \text{span}\{\psi_i\}_{i\in\Omega}. \quad (\text{A.5})$$

Approximation by thresholding can be interpreted as the orthogonal projection of x onto the nearest subspace in Σ_K , a simple but nonlinear technique owing to the nonlinear geometry of Σ_K .

A few questions leading to CS theory are as follows:

- How to find the nearest Σ_K ?
- Can a non-adaptive, linear method assure dimensionality reduction?

A.3 Compressive Sensing

For an n -dimensional vector $x \in \mathcal{R}^N$, where N is large, compressive measurements $y \in \mathcal{R}^M$, where $M \ll N$ are obtained as

$$y = \Phi x. \quad (\text{A.6})$$

Φ is called as measurement matrix. In general, it is an impossible task to find x given y and Φ as M samples of y yield a $(N - M)$ dimensional subspace of possible solutions for the original x that would match our given observations. In other words, as Φ is rank deficient. As it has non-empty null-space, one can get $y = \Phi x_1 = \Phi x_2$. However, CS attempts to recover the sparse x , out of all possible x . A vector x is K -sparse if it has at most K non-zero coefficients in that basis (i.e. $\|x\|_0 \leq K$, where $\|\cdot\|_0$ denotes the l_0 norm). A signal x has to be sparse either in time domain or under some sparsifying transform Ψ (at least approximately, if not exactly). Thus, we restrict ourselves to Σ_K , the class of all K -sparse signals. We can now write measurement process as

$$y = \Phi \Psi \tilde{x} = \Theta x. \quad (\text{A.7})$$

Here $\tilde{x} = \Psi^T x$, i.e. transformed vector. Traditional techniques for solving for x (e.g., inversion, least squares) do not work because (A.7) is severely under-determined (since $M \ll N$). However, advances in CS have shown that if $M \geq 2K$ and Θ meets certain properties, then (A.7) can be solved uniquely for x , by looking for the sparsest x that satisfies the equation. The CS recovery problem is stated as

$$P0 : \hat{x} = \arg \min \|x\|_0 \text{ such that } y = \Theta x. \quad (\text{A.8})$$

The solution to this problem, however, involves a combinatorial algorithm in which every x with $\|x\|_0 \leq K$ is checked to find the one that results in the measured samples y . This problem is known to be Nondeterministic-Polynomial-Time (NP) Complete for any practical signal. However, recent results have shown that (A.8) can be solved by introducing convex relaxation as below

$$P1 : \hat{x} = \arg \min \|x\|_1 \text{ such that } y = \Theta x \quad (\text{A.9})$$

where l_1 -norm $\|x\|_1 = \sum_{i=1}^n |x_i|$.

As long as the number of samples $m = O(k \log n)$ and the matrix Φ meets the restricted isometry property (RIP) with parameters $(2k, \sqrt{2} - 1)$, solutions to the $P0$ and $P1$ problems are same.

A.3.1 Restricted Isometry Property (RIP)

One cannot solve $y = \Theta x$ for x with any arbitrary Φ ($M \ll N$), even if $M \geq 2K$. However, recovery of x is guaranteed if matrix Φ meets the Restricted Isometry Property (RIP), stated as

$$(1 - \epsilon)\|v\|_2 \leq \|\Theta v\|_2 \leq (1 + \epsilon)\|v\|_2 \quad (\text{A.10})$$

with parameters (K, ϵ) , where $\epsilon \in (0, 1)$ for all K -sparse vectors v . Essentially, the RIP states that a measurement matrix will be valid if every possible set of K columns of Θ form an approximate orthogonal set. Another way to state this is, if $x, x' \in \Sigma_K$ and $x \neq x'$ then, $\Phi x \neq \Phi x'$. That is, the distances are preserved even after projection. Further, we want the sampling matrix Φ to be as incoherent to the compression basis Ψ as possible. Examples of matrices that have been proven to meet RIP with very high probability include Gaussian matrices, Bernoulli matrices and partial Fourier matrices.

The sampling matrices used in this work are:

- Sparse random matrices whose entries are sampled from Gaussian distribution.
- Row restrictions of identity matrices. Indices of the rows to be kept come from random permutations.
- Row restrictions of identity matrices. Instead of completely random restrictions, we chose random indices in uniform bins. For example, if one wants to keep a fraction $1/d$ of total samples randomly, one chooses a number from every non overlapping consecutive partitions of length d in $[1, N]$, where N is the number of rows.

A.3.2 Greedy Reconstruction Algorithms

Owing to simplicity, one often attempts to solve (A.8) using greedy algorithms. Orthogonal Matching Pursuit (OMP) has proved to be one of the most successful greedy algorithms [55]. Given the measured vector y and the measurement matrix Φ , one finds the coefficient of x with the largest magnitude by projecting \tilde{x} onto each column of A and selecting the largest $\langle \tilde{x}, a_j \rangle$, where a_j is the j th column of A . Once such coefficient is identified, a least-squares problem is solved assuming it is the only non-zero coefficient. The new estimate for \hat{x} is used to compute the estimated signal x . The algorithm is iterated using the residual to solve for the next largest coefficient of \hat{x} one at a time. By iterating k times, one finds an k -sparse approximation of the transform domain vector.

A.4 Dictionary Learning

The method of dictionary learning identifies a tunable selection of basis vectors providing sparse representation to the given set of signals.

Given a set of signals $\{x_i\}_{i=1}^N$, K -SVD [51] seeks the dictionary D that provides the sparsest representation for each example in this set. To begin with, for some arbitrary dictionary D , the

method starts finding the matrix Ψ , each of whose columns is sparse enough, from the following optimization problem

$$\Psi = \arg \min_{\Theta} \sum_l \|\Theta_l\|_1 \text{ subject to } X = D\Theta. \quad (\text{A.11})$$

where Θ_l is the l^{th} column of Θ . Using Ψ , the pair (D, Ψ) is then updated as follows:

$$(\hat{D}, \hat{\Psi}) = \arg \min_{D, \Psi} \|X - D\Psi\|_F^2 \text{ subject to } \|\gamma_i\|_0 \leq T_0 \forall i. \quad (\text{A.12})$$

where γ_i represents the i^{th} column of Ψ , X is the matrix whose columns are x_i and T_0 is the sparsity parameter. Here, $\|A\|_F$ denotes the Frobenius norm and is defined as $\|A\|_F = \sqrt{\sum_{ij} A_{ij}^2}$. The K -SVD algorithm alternates between the sparse coding (A.11), solved using an ℓ_1 solver such as OMP, and dictionary update (A.12), requiring least square methods, till there is a convergence in the dictionaries so learnt.

References

- [1] “World Health Organization, Fact Sheet on CVDs (Fact Sheet N^o317),” Mar. 2013. (<http://www.who.int/mediacentre/factsheets/fs317/en/>)
- [2] L. Sörnmo, P. Laguna, “Bioelectrical Signal Processing in Cardiac and Neurological Applications”, *Academic Press*, 2005.
- [3] B. S. Chandra, C. S. Sastry, S. Jana, “Telecardiology: Hurst Exponent based Anomaly Detection in Compressively Sampled ECG Signals,” *IEEE 15th International Conference on e-Health Networking, Applications, Services (Healthcom)*, pp. 350–354, Oct. 2013.
- [4] S. Maheshwari, A. Acharyya, P. E. Puddu, M. Schiariti, “Reduced Lead System Selection Methodology for Reliable Standard 12-Lead Reconstruction Targeting Personalized Remote Health Monitoring Applications,” *Computer Methods in Biomechanics and Biomedical Engineering: Imaging & Visualization*, vol. 2, no. 2, pp. 107–120, 2014.
- [5] D. Craven, B. McGinley, L. Kilmartin, M. Glavin, E. Jones, “Compressed Sensing for Bioelectric Signals: A Review,” *IEEE Journal of Biomedical and Health Informatics*, 2014.
- [6] S. Jalaaliddine, C. Hutchens, R. Strattan, W. Coberly, “ECG Data Compression Techniques – A Unified Approach,” *IEEE Transactions on Biomedical Engineering*, vol. 37, no. 4, pp. 329–343, Apr. 1990.
- [7] M. Shridhar, N. Mohankrishnan, “Data Compression Techniques for Electrocardiograms,” *Canadian Electrical Engineering Journal*, vol. 9, no. 4, pp. 126–131, Oct. 1984.
- [8] U. E. Ruttimann, H. V. Pipberger, “Compression of the ECG by Prediction or Interpolation and Entropy Encoding,” *IEEE Transactions on Biomedical Engineering*, vol. BME-26, no. 11, pp. 613–623, Nov. 1979.
- [9] H. Baali, M. Salami, R. Akmeliawati, A. Aibinu, “Analysis of the ECG Signal using SVD-based Parametric Modeling Technique,” *Sixth IEEE International Symposium on Electronic Design, Test and Application (DELTA)*, pp. 180–184, Jan. 2011.
- [10] C. Lamberti, M. Zagnoni, R. Degani, G. Bortolan, “Evaluation of Algorithms for Real-time ECG Data Compression,” *Proceedings of Computers in Cardiology*, pp. 399–402, Sep. 1990.
- [11] K. Akazawa, T. Uchiyama, S. Tanaka, A. Sasamori, E. Harasawa, “Adaptive Data Compression of Ambulatory ECG using Multi Templates,” *Proceedings of Computers in Cardiology*, pp. 495–498, Sep. 1993.

- [12] S. Cannon, L. Widman, "An Equal Compression-Ratio Comparison of Beat-to-beat and SAPA2 Compression Techniques," *Proceedings of Computers in Cardiology*, pp. 675–678, Oct. 1992.
- [13] M. Evin, M. Korurek, "A New Data Compression Technique for Electrocardiograms," *International Biomedical Engineering Days*, pp. 61–63, Aug. 1992.
- [14] P. S. Hamilton, "A Comparison of Algorithms for Ambulatory ECG Compression with Fixed Average Data Rate," *Proceedings of Computers in Cardiology*, pp. 683–686, Oct. 1992.
- [15] B. Reddy, I. Murthy, "ECG Data Compression Using Fourier Descriptors," *IEEE Transactions on Biomedical Engineering*, vol. BME-33, no. 4, pp. 428–434, Apr. 1986.
- [16] N. Ahmed, P. J. Milne, S. G. Harris, "Electrocardiographic Data Compression via Orthogonal Transforms," *IEEE Transactions on Biomedical Engineering*, vol. BME-22, no. 6, pp. 484–487, Nov. 1975.
- [17] M. Womble, J. Halliday, S. Mitter, M. C. Lancaster, J. H. Triebwasser, "Data Compression for Storing and Transmitting ECGs/VCGs," *Proceedings of the IEEE*, vol. 65, no. 5, pp. 702–706, May 1977.
- [18] R. Degani, G. Bortolan, R. Murolo, "Karhunen-Loeve Coding of ECG Signals," *Proceedings of Computers in Cardiology*, pp. 395–398, Sep. 1990.
- [19] T. Kiryu, N. Kodaira, H. Ogawa, Y. Saitoh, "ECG Data Compression by Biorthogonal Basis," *16th Annual International Conference of the IEEE EMBS Engineering Advances: New Opportunities for Biomedical Engineers*, vol. 2, pp. 1266–1267, 1994.
- [20] R. Benzid, F. Marir, A. Boussaad, M. Benyoucef, D. Arar, "Fixed Percentage of Wavelet Coefficients to be Zeroed for ECG Compression," *Electronics Letters*, vol. 39, no. 11, pp. 830–831, May 2003.
- [21] M. Unser, A. Aldroubi, "A Review of Wavelets in Biomedical Applications," *Proceedings of the IEEE*, vol. 84, no. 4, pp. 626–638, Apr. 1996.
- [22] M. Abo-Zahhad, B. Rajoub, "ECG Compression Algorithm Based on Coding and Energy Compaction of the Wavelet Coefficients," *The 8th IEEE International Conference on Electronics, Circuits and Systems*, vol. 1, pp. 441–444, 2001.
- [23] M. Abo-Zahhad, S. Ahmed, A. Al-Shrouf, "Electrocardiogram Data Compression Algorithm based on the Linear Prediction of the Wavelet Coefficients," *The 7th IEEE International Conference on Electronics, Circuits and Systems*, vol. 1, pp. 599–603, 2001.
- [24] M. Hilton, "Wavelet and Wavelet Packet Compression of Electrocardiograms," *IEEE Transactions on Biomedical Engineering*, vol. 44, no. 5, pp. 394–402, May 1997.
- [25] Z. Lu, D. Y. Kim, W. Pearlman, "Wavelet Compression of ECG Signals by the Set Partitioning in Hierarchical Trees Algorithm," *IEEE Transactions on Biomedical Engineering*, vol. 47, no. 7, pp. 849–856, Jul. 2000.

- [26] L. Polania, R. Carrillo, M. Blanco-Velasco, K. Barner, “Compressed Sensing Based Method for ECG Compression,” *IEEE International Conference on Acoustics, Speech and Signal Processing*, pp. 761–764, May 2011.
- [27] A. Tuzman, S. Chialanza, “Design of Wavelet Basis for ECG Compression,” *Proceedings of the 20th Annual International Conference of the IEEE EMBS*, vol. 1, pp. 198–201, Oct. 1998.
- [28] A. Tuzman, S. Chialanza, M. Acosta, R. Bartesaghi, T. Hobbins, A. Fonseca, “Best Wavelet Basis Design for Joint Compression–Classification of Long ECG Data Records,” *Computers in Cardiology*, pp. 287–290, Sep. 1997.
- [29] B. N. Singh, A. K. Tiwari, “Optimal Selection of Wavelet Basis Function Applied to {ECG} Signal Denoising,” *Digital Signal Processing*, vol. 16, no. 3, pp. 275–287, 2006.
- [30] R. Besar, C. Eswaran, S. Sahib, R. Simpson, “On the Choice of the Wavelets for ECG Data Compression,” *IEEE International Conference on Acoustics, Speech, and Signal Processing*, vol. 6, 2000, pp. 3614–3617.
- [31] R. R. Tamboli, M. Savkooor, S. Jana, R. Manthalkar, “On the Sparsest Representation of Electrocardiograms,” *Computing in Cardiology Conference (CinC)*, pp. 479–482, Sep. 2013.
- [32] H. Mamaghanian, N. Khaled, D. Atienza, P. Vandergheynst, “Compressed Sensing for Real–Time Energy–Efficient ECG Compression on Wireless Body Sensor Nodes,” *IEEE Transactions on Biomedical Engineering*, vol. 58, no. 9, pp. 2456–2466, Sep. 2011.
- [33] S. Rabiul, X. Huang, D. Sharma, “Wavelet Based Denoising Algorithm of the ECG Signal Corrupted by WGN and Poisson Noise,” *International Symposium on Communications and Information Technologies (ISCIT)*, pp. 165–168, 2012.
- [34] Z. Lu, D. Y. Kim, W. Pearlman, “ECG Signal Compression With A New Wavelet Method,” *Proceedings of the First Joint BMES/EMBS Conference*, vol. 2, pp. 955, Oct. 1999.
- [35] K. Kanoun, H. Mamaghanian, N. Khaled, D. Atienza, “A Real–Time Compressed Sensing–Based Personal Electrocardiogram Monitoring System,” *Design, Automation Test in Europe Conference Exhibition*, pp. 1–6, Mar. 2011.
- [36] A. Dixon, E. Allstot, D. Gangopadhyay, D. Allstot, “Compressed Sensing System Considerations for ECG and EMG Wireless Biosensors,” *IEEE Transactions on Biomedical Circuits and Systems*, vol. 6, no. 2, pp. 156–166, Apr. 2012.
- [37] D. S. Reddy, R. R. Tamboli, and S. Jana, “Universal Nonuniform Sampling of ECG Signals: Opportunities and Obstacles,” *Biomedical Engineering International Conference (BMEiCON)*, pp. 1–5, Dec 2012.
- [38] M. D. Menz, “Minimum Sampling Rate in Electrocardiology,” *Journal of Clinical Engineering*, vol. 19, no. 5, pp. 386–394, 1994.
- [39] B. Huang, W. Kinsner, “Impact of Low–Rate Sampling on the Reconstruction of ECG in Phase–Space,” *Canadian Conference on Electrical and Computer Engineering*, vol. 1, pp. 508–512, 2000.

- [40] F. Simon, J. Martinez, P. Laguna, B. van Grinsven, C. Rutten, R. Houben, "Impact of Sampling Rate Reduction on Automatic ECG Delineation," *29th Annual International Conference of the IEEE EMBS*, pp. 2587–2590, Aug. 2007.
- [41] P. Castiglioni, L. Piccini, M. Di Rienzo, "Interpolation Technique for Extracting Features from ECG Signals Sampled At Low Sampling Rates," *Computers in Cardiology*, pp. 481–484, 2003.
- [42] A. L. Goldberger, L. A. Amaral, L. Glass, J. M. Hausdorff, P. C. Ivanov, R. G. Mark, J. E. Mietus, G. B. Moody, C.K. Peng, H. E. Stanley, "Physiobank, Physiokit, Physionet: Components of a New Research Resource for Complex Physiologic Signals," *Circulation*, vol. 101, no. 23, pp. e215–e220, 2000.
- [43] A. Alesanco, J. Garcia, "Automatic Real-Time ECG Coding Methodology Guaranteeing Signal Interpretation Quality," *IEEE Transactions on Biomedical Engineering*, vol. 55, no. 11, pp. 2519–2527, Nov. 2008.
- [44] L. Sharma, S. Dandapat, A. Mahanta, "Multichannel ECG Data Compression based on Multiscale Principal Component Analysis," *IEEE Transactions on Information Technology in Biomedicine*, vol. 16, no. 4, pp. 730–736, Jul. 2012.
- [45] Y. Zigel, A. Cohen, A. Katz, "The Weighted Diagnostic Distortion (WDD) Measure for ECG Signal Compression," *IEEE Transactions on Biomedical Engineering*, vol. 47, no. 11, pp. 1422–1430, Nov. 2000.
- [46] Y. Zigel, A. Cohen, A. Katz, "ECG Signal Compression using Analysis by Synthesis Coding," *IEEE Transactions on Biomedical Engineering*, vol. 47, no. 10, pp. 1308–1316, Oct. 2000.
- [47] R. R. Tamboli, D. S. Reddy, S. Jana, "A Hybrid Fourier/ Wavelet Technique for Improved ECG Signal Approximation," *IEEE International Conference on Signal Processing, Computing and Control (ISPCC)*, pp. 1–6, Sep. 2013.
- [48] J. Rissanen, "Modeling by Shortest Data Description," *Automatica*, vol. 14, no. 5, pp. 465–471, 1978.
- [49] A. Bendifallah, R. Benzid, M. Boulemden, "Improved ECG Compression Method using Discrete Cosine Transform," *Electronics Letters*, vol. 47, no. 2, pp. 87–89, Jan. 2011.
- [50] S. Jana, P. Moulin, "Optimality of KLT for High-Rate Transform Coding of Gaussian Vector-Scale mixtures: Application to Reconstruction, Estimation and Classification," *IEEE Transactions on Information Theory*, vol. 52, no. 9, pp. 4049–4067, Sep. 2006.
- [51] M. Aharon, M. Elad, A. Bruckstein, "K-SVD: An Algorithm for Designing Overcomplete Dictionaries for Sparse Representation," *IEEE Transactions on Signal Processing*, vol. 54, no. 11, pp. 4311–4322, 2006.
- [52] S. J. Lee, J. Luan, P. H. Chou, "ECG Signal Reconstruction from Undersampled Measurement using A Trained Overcomplete Dictionary," *4th International Conference on Convergence and its Applications*, 2014.

- [53] A. V. Oppenheim, R. W. Schaffer, J. R. Buck *et al.*, *Discrete-Time Signal Processing*, Prentice-Hall Englewood Cliffs, vol. 2, 1989.
- [54] E. Candes, M. Wakin, “An Introduction to Compressive Sampling,” *IEEE Signal Processing Magazine*, vol. 25, no. 2, pp. 21–30, Mar. 2008.
- [55] J. Tropp, A. Gilbert, “Signal Recovery from Random Measurements via Orthogonal Matching Pursuit,” *IEEE Transactions on Information Theory*, vol. 53, no. 12, pp. 4655–4666, Dec. 2007.
- [56] D. Needell, R. Vershynin, “Signal Recovery from Incomplete and Inaccurate Measurements via Regularized Orthogonal Matching Pursuit,” *IEEE Journal of Selected Topics in Signal Processing*, vol. 4, no. 2, pp. 310–316, Apr. 2010.
- [57] C. Shannon, “A Mathematical Theory of Communication,” *The Bell System Technical Journal*, vol. 27, no. 3, pp. 379–423, Jul. 1948.
- [58] R. G. Baraniuk, V. Cevher, M. F. Duarte, C. Hegde, “Model-Based Compressive Sensing,” *IEEE Transactions on Information Theory*, vol. 56, no. 4, pp. 1982–2001, 2010.